INSTITUTE OF PHYSICS PUBLISHING WAVES IN RANDOM MEDIA

Waves Random Media **14** (2004) 229–252 PII: S0959-7174(04)69410-9

# Multiple scattering in the high-frequency limit with second-order shadowing function from 2D anisotropic rough dielectric surfaces: I. Theoretical study

**C Bourlier**[1] **and G Berginc**[2]

[1] IREENA, Radar Team, Ecole polytechnique de l'université de Nantes—Bat. IRESTE, Rue Christian Pauc, La Chantrerie, BP 50609, 44306 Nantes Cedex 3, France
[2] DS/DFO, THALES Optronique, Rue Guynemer BP 55, 78283 Guyancourt Cedex, France

E-mail: christophe.bourlier@polytech.univ-nantes.fr

Received 23 September 2003, in final form 19 February 2004
Published 31 March 2004
Online at stacks.iop.org/WRM/14/229 (DOI: 10.1088/0959-7174/14/3/003)

**Abstract**

In this paper the first- and second-order Kirchhoff approximation is applied to study the backscattering enhancement phenomenon, which appears when the surface rms slope is greater than 0.5. The formulation is reduced to the geometric optics approximation in which the second-order illumination function is taken into account. This study is developed for a two-dimensional (2D) anisotropic stationary rough dielectric surface and for any surface slope and height distributions assumed to be statistically even. Using the Weyl representation of the Green function (which introduces an absolute value over the surface elevation in the phase term), the incoherent scattering coefficient under the stationary phase assumption is expressed as the sum of three terms. The incoherent scattering coefficient then requires the numerical computation of a ten- dimensional integral. To reduce the number of numerical integrations, the geometric optics approximation is applied, which assumes that the correlation between two adjacent points is very strong. The model is then proportional to two surface slope probabilities, for which the slopes would specularly reflect the beams in the double scattering process. In addition, the slope distributions are related with each other by a propagating function, which accounts for the second-order illumination function. The companion paper is devoted to the simulation of this model and comparisons with an 'exact' numerical method.

## 1. Introduction

One of the most interesting phenomena associated with rough-surface scattering is the backscattering enhancement effect [1]. This phenomenon is associated with the appearance

  

of a well-defined peak in the backscattering direction of the intensity of the incoherently scattered component of the electromagnetic field. Enhanced backscattering has been observed experimentally [2–5] and numerically [6–8] from the numerical Monte Carlo method. The enhanced backscattering phenomenon can involve surfaces with relatively large slopes for which predictions of the standard Kirchhoff approximation and of the small perturbation method of first order are inaccurate, because of the small slope limitations of these approximate theories. However, other approximate theories such as a higher-order Kirchhoff approximation [9], the IEM (integral equation model) [10], full-wave method [11] for surfaces with large slope have been developed to explain the backscattering enhancement phenomenon. They remain restricted to their domains of validity and the random surface is assumed to be Gaussian as the numerical method. In addition, these analytical theories include the shadowing effects from the shadowing function with single reflection. Recently, Bourlier *et al* gave a rigorous formulation of the shadowing effect with double reflection [12].

In this paper, for any random two-dimensional (2D) anisotropic dielectric surfaces assumed to be statistically even, the incoherent scattering coefficient is derived from the first- and second-order Kirchhoff approximation reduced to the geometric optics approximation. Moreover, the second-order shadowing function is included. The formulation is based on the work of Ishimaru *et al* [9] with the following differences:

- From the Weyl representation, Ishimaru *et al* expanded the Green function over the difference of the horizontal distance $|x_2 - x_1|$, whereas we expand it over the height difference $|z_2 - z_1|$ such as the IEM model [13, 14].
- For the calculation of the second-order illumination function, Ishimaru *et al* used the shadowing function with single reflection from a geometrical procedure, whereas we use a recently published rigorous formulation [12].
- Ishimaru *et al* assumed a Gaussian process for the surface, whereas our formulation is valid for any random process.
- Ishimaru *et al* assumed an isotropic surface, whereas we consider an anisotropic surface.
- Ishimaru *et al* neglected the cross Kirchhoff term whereas we derive its contribution.

The paper is organized as follows. In section 2, the first- and second-order Kirchhoff approximation is addressed and in section 3, the incoherent scattering coefficient is derived under the geometric optics approximation for any random process. In section 4, the shadowing effect is incorporated in the incoherent scattering coefficient and the last section gives concluding remarks. In the companion paper, the model will be simulated for co- and cross polarizations and will be compared with an 'exact' numerical method.

## 2. Formulation of the first- and second-order Kirchhoff approximations

In this section, the first- and second-order Kirchhoff approximations combined with the stationary phase approximation are presented to calculate the bistatic cross-section of waves scattered from two- dimensional randomly rough surfaces. In the first and second subsections, the first- and second-order Kirchhoff fields are addressed and in the last subsection the average scattered power is performed.

### *2.1. First-order Kirchhoff approximation*

The first-order Kirchhoff approximation has been studied extensively in the past. Here a brief summary is presented.

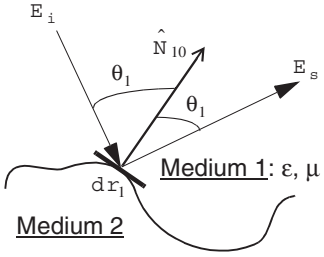


**Figure 1.** First-order Kirchhoff approximation.

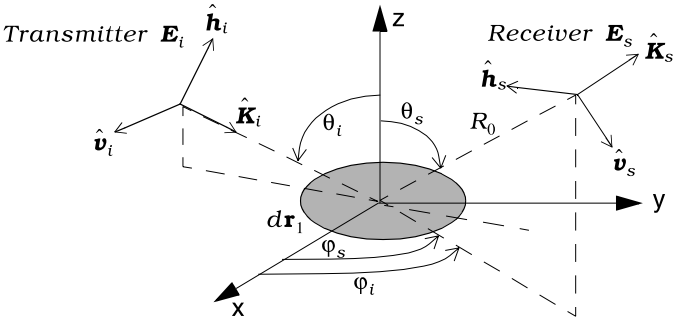


**Figure 2.** Geometry of the problem for the first-order Kirchhoff approximation.

With the Kirchhoff approach, the scattered field is written in terms of the tangential field on a rough surface (see figure 1). The surface field is then approximated by the field that would be present if the rough surface was replaced by a planar surface tangential to the point of interest. This means that the surface total scattered field can be expressed from the incident field $\boldsymbol{E}_i = E_0\hat{\boldsymbol{a}}\exp(\mathrm{j}\boldsymbol{K}_i\cdot\boldsymbol{R}_1)$ and the Fresnel coefficients $\{F_V, F_H\}$ for $V$ and $H$ polarizations, respectively. $\hat{\boldsymbol{a}}$ is the unitary polarization vector of the incident field of direction $\boldsymbol{K}_i$. The Fresnel coefficients are determined with an angle $\theta_1 = -\arccos(\hat{\boldsymbol{N}}_1\cdot\hat{\boldsymbol{K}}_i)$ where $\hat{\boldsymbol{K}}_i = \boldsymbol{K}_i/k_0$, for which $k_0$ is the incident wavenumber. $\hat{\boldsymbol{N}}_1$ is the unitary vector normal to the surface.

The total scattered field in the far-field zone is then expressed as follows [15]:

$$\boldsymbol{E}_s = \mathrm{j}k_0E_0\int \boldsymbol{F}(\hat{\boldsymbol{N}}_1,\hat{\boldsymbol{K}}_i,\hat{\boldsymbol{K}}_s)G(\boldsymbol{R}_1,\boldsymbol{R})\exp(\mathrm{j}\boldsymbol{K}_i\cdot\boldsymbol{R}_1)\,\mathrm{d}\boldsymbol{r}_1, \tag{1}$$

where

$$\begin{aligned}\boldsymbol{F}(\hat{\boldsymbol{N}}_1,\hat{\boldsymbol{K}}_i,\hat{\boldsymbol{K}}_s) &= \hat{\boldsymbol{K}}_s\wedge[(1+F_H)(\hat{\boldsymbol{a}}\cdot\hat{\boldsymbol{t}})(\hat{\boldsymbol{N}}_1\wedge\hat{\boldsymbol{t}}) - (1-F_V)(\hat{\boldsymbol{N}}_1\cdot\hat{\boldsymbol{K}}_i)(\hat{\boldsymbol{a}}\cdot\hat{\boldsymbol{d}})\hat{\boldsymbol{t}}]\\ &\quad+\hat{\boldsymbol{K}}_s\wedge\hat{\boldsymbol{K}}_s\wedge[(1+F_V)(\hat{\boldsymbol{a}}\cdot\hat{\boldsymbol{d}})(\hat{\boldsymbol{N}}_1\wedge\hat{\boldsymbol{t}}) + (1-F_H)(\hat{\boldsymbol{N}}_1\cdot\hat{\boldsymbol{K}}_i)(\hat{\boldsymbol{a}}\cdot\hat{\boldsymbol{t}})\hat{\boldsymbol{t}}],\end{aligned} \tag{1a}$$

and

$$\boldsymbol{R}_1 = x_1\hat{\boldsymbol{x}} + y_1\hat{\boldsymbol{y}} + z_1\hat{\boldsymbol{z}} = \boldsymbol{r}_1 + z_1\hat{\boldsymbol{z}}. \tag{1b}$$

The unitary vectors $\{\hat{\boldsymbol{t}},\hat{\boldsymbol{d}}\}$ are defined as $\hat{\boldsymbol{t}} = \hat{\boldsymbol{K}}_i\wedge\hat{\boldsymbol{N}}_1/\|\hat{\boldsymbol{K}}_i\wedge\hat{\boldsymbol{N}}_1\|$, $\hat{\boldsymbol{d}} = \hat{\boldsymbol{K}}_i\wedge\hat{\boldsymbol{t}}$ and $G(\boldsymbol{R}_1,\boldsymbol{R})$ denotes the scalar Green function, which can be approximated in the far-field zone as

$$G(\boldsymbol{R}_1,\boldsymbol{R}) = \exp(\mathrm{j}k_0R_0 - \mathrm{j}\boldsymbol{K}_s\cdot\boldsymbol{R}_1)/(4\pi R_0), \tag{2}$$

where $R_0$ range from the surface to the receiver.

The stationary phase method is commonly used to evaluate the scattered field over a rough surface. This approach assumes that the major contribution of the scattered field from the rough surface comes from the regions around the specular direction. This means that the normal to the surface $\hat{\boldsymbol{N}}_1 = \hat{\boldsymbol{N}}_{10}$ becomes independent of the surface slopes

$$\hat{\boldsymbol{N}}_{10} = (\boldsymbol{K}_s - \boldsymbol{K}_i)/\|\boldsymbol{K}_s - \boldsymbol{K}_i\|. \tag{3}$$

Let $\hat{\boldsymbol{v}}_i, \hat{\boldsymbol{h}}_i$ be unitary polarization vectors for the incident and horizontal waves, respectively. Let $\hat{\boldsymbol{v}}_s, \hat{\boldsymbol{h}}_s$ be the corresponding polarization vectors for the scattered waves. The unitary vectors $\{\hat{\boldsymbol{K}}_i, \hat{\boldsymbol{h}}_i, \hat{\boldsymbol{v}}_i, \hat{\boldsymbol{K}}_s, \hat{\boldsymbol{h}}_s, \hat{\boldsymbol{v}}_s\}$ (see figure 2) are defined as follows [15]:

$$\hat{\boldsymbol{K}}_i = \sin\theta_i\cos\varphi_i\hat{\boldsymbol{x}} + \sin\theta_i\sin\varphi_i\hat{\boldsymbol{y}} - \cos\theta_i\hat{\boldsymbol{z}},\ \hat{\boldsymbol{h}}_i = -\sin\varphi_i\hat{\boldsymbol{x}} + \cos\varphi_i\hat{\boldsymbol{y}},\ \hat{\boldsymbol{v}}_i = \hat{\boldsymbol{h}}_i \wedge \hat{\boldsymbol{K}}_i, \tag{4}$$

and

$$\hat{\boldsymbol{K}}_s = \sin\theta_s\cos\varphi_s\hat{\boldsymbol{x}} + \sin\theta_s\sin\varphi_s\hat{\boldsymbol{y}} + \cos\theta_s\hat{\boldsymbol{z}},\ \hat{\boldsymbol{h}}_s = -\sin\varphi_s\hat{\boldsymbol{x}} + \cos\varphi_s\hat{\boldsymbol{y}},\ \hat{\boldsymbol{v}}_i = \hat{\boldsymbol{h}}_s \wedge \hat{\boldsymbol{K}}_s. \tag{5}$$

When the incident wave is horizontally polarized, in (1$a$) $\hat{\boldsymbol{a}} = \hat{\boldsymbol{h}}_i$. The co- and cross scattered fields are then given by $E_s^{h_i h_s} = \hat{\boldsymbol{h}}_s \cdot \hat{\boldsymbol{E}}_s$, and $E_s^{h_i v_s} = \hat{\boldsymbol{v}}_s \cdot \boldsymbol{E}_s$, respectively. In the same way where $\hat{\boldsymbol{a}} = \hat{\boldsymbol{v}}_i$, $E_s^{v_i h_s} = \hat{\boldsymbol{h}}_s \cdot \boldsymbol{E}_s$ and $E_s^{v_i v_s} = \hat{\boldsymbol{v}}_s \cdot \boldsymbol{E}_s$ are obtained. Substituting (3) into (1$a$) and (2) into (1), according to the polarization states of the incident $i = \{v_i, h_i\}$ and scattered $s = \{v_s, h_s\}$ fields, the components of the scattered field are

$$E_s^{i\to s} = \frac{\mathrm{j}k_0\exp(\mathrm{j}k_0R_0)}{4\pi R_0} E_0 I_1 \bar{F}_1(\hat{\boldsymbol{K}}_i, \hat{\boldsymbol{K}}_s), \tag{6}$$

where

$$I_1 = \int \Xi_1(\mathbf{r}_1)\exp[-j(\boldsymbol{K}_s - \boldsymbol{K}_i)\cdot\boldsymbol{R}_1]\,\mathrm{d}\mathbf{r}_1. \tag{6a}$$

The square matrix $\bar{F}_1(\hat{\boldsymbol{K}}_i, \hat{\boldsymbol{K}}_s)$ of length 2 is given in appendix A. In (6$a$), $\Xi_1(\mathbf{r}_1)$ denotes the one- order illumination function; $\Xi_1(\mathbf{r}_1) = 1$ if the point corresponding to $\mathbf{r}_1$ is illuminated and the rays emanating from the transmitter and receiver do not cross the surface, $\Xi_1(\mathbf{r}_1) = 0$ else. The term $I_1$ depends on the position $\mathbf{r}_1$ and on the surface elevation $z_1 = z(\mathbf{r}_1)$ through $\boldsymbol{R}_1 = \mathbf{r}_1 + z_1\hat{\boldsymbol{z}}$.

### 2.2. *Second-order Kirchhoff approximation*

As depicted in figure 3, the field at $\mathbf{r}_2$ consists of the first- and second-order Kirchhoff approximations. The second-order Kirchhoff field $\boldsymbol{E}_2$ at $\mathbf{r}_2$ is obtained using the first-order Kirchhoff approximation at $\mathbf{r}_1$ and propagating from $\mathbf{r}_1$ to $\mathbf{r}_2$.

By analogy with (1), the components of the field $E_1^{i\to m}$ scattered from $\mathbf{r}_1$ and propagating towards $\mathbf{r}_2$ with respect to $\hat{\boldsymbol{K}}_m$ can be expressed as

$$E_1^{i\to m} = \mathrm{j}k_0E_0\int \bar{F}(\hat{\boldsymbol{N}}_1, \hat{\boldsymbol{K}}_i, \hat{\boldsymbol{K}}_m)G(\boldsymbol{R}_1, \boldsymbol{R}_2)\exp(\mathrm{j}\boldsymbol{K}_i\cdot\boldsymbol{R}_1)\,\mathrm{d}\mathbf{r}_1, \tag{7}$$

where $\hat{\boldsymbol{K}}_m = \boldsymbol{K}_m/k_0$, for which

$$\hat{\boldsymbol{K}}_m = \hat{\boldsymbol{k}} + m\hat{q}\hat{\boldsymbol{z}} = \sin\theta\cos\varphi\hat{\boldsymbol{x}} + \sin\theta\sin\varphi\hat{\boldsymbol{y}} + m\cos\theta\hat{\boldsymbol{z}}, \qquad \text{where}$$
$$m = \pm 1 = \mathrm{sign}(z_2 - z_1). \tag{7a}$$

The polarization basis is $i = \{v_i, h_i\}$ for the emitter and $m = \{v_m, h_m\}$ for the scattered field propagating with respect to $\hat{\boldsymbol{K}}_m$.

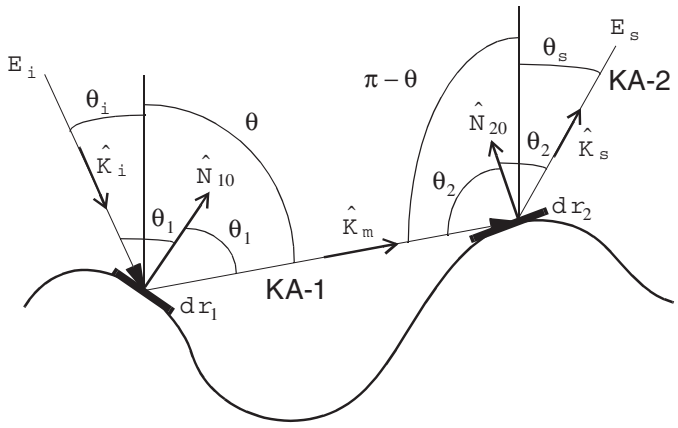


**Figure 3.** Illustration of the second-order Kirchhoff approximation denoted as KA-2.

In the same way, the components of the scattered field $E_s^{i\to s}$ from $\mathbf{r}_2$ are expressed from $E_1^{i\to m}$ as

$$E_s^{i\to s} = \mathrm{j}k_0 \int E_1^{i\to m} G(\boldsymbol{R}_2, \boldsymbol{R}) \bar{F}(\hat{\boldsymbol{N}}_2, \hat{\boldsymbol{K}}_{-m}, \hat{\boldsymbol{K}}_s)\, \mathrm{d}\mathbf{r}_2$$
$$= (\mathrm{j}k_0)^2 E_0 \int \bar{F}_m G(\boldsymbol{R}_1, \boldsymbol{R}_2) G(\boldsymbol{R}_2, \boldsymbol{R}) \exp(\mathrm{j}\boldsymbol{K}_i \cdot \boldsymbol{R}_1)\, \mathrm{d}\mathbf{r}_1\, \mathrm{d}\mathbf{r}_2, \tag{8}$$

where

$$\bar{F}_m = \bar{F}(\hat{\boldsymbol{N}}_1, \hat{\boldsymbol{K}}_i, \hat{\boldsymbol{K}}_m) \times \bar{F}(\hat{\boldsymbol{N}}_2, \hat{\boldsymbol{K}}_{-m}, \hat{\boldsymbol{K}}_s). \tag{8a}$$

$\bar{F}_m$ is a square matrix of length 2 calculated from a product matrix of $\bar{F}(\hat{\boldsymbol{N}}_1, \hat{\boldsymbol{K}}_i, \hat{\boldsymbol{K}}_m)$ and $\bar{F}(\hat{\boldsymbol{N}}_2, \hat{\boldsymbol{K}}_{-m}, \hat{\boldsymbol{K}}_s)$. Since the scattered field $E_s^{i\to s}$ is derived in the far zone, we have

$$G(\boldsymbol{R}_2, \boldsymbol{R}) = \exp(\mathrm{j}k_0 R_0 - \mathrm{j}\boldsymbol{K}_s \cdot \boldsymbol{R}_2)/(4\pi R_0). \tag{9}$$

The expansion of the retarded Green function $G(\boldsymbol{R}_1, \boldsymbol{R}_2)$ into plane waves is called the Weyl representation of a spherical wave

$$G(\boldsymbol{R}_1, \boldsymbol{R}) = \frac{\mathrm{j}}{8\pi^2} \int \frac{1}{q} \exp\{\mathrm{j}[\boldsymbol{k} \cdot (\mathbf{r}_2 - \mathbf{r}_1) + q|z_2 - z_1|]\}\, \mathrm{d}\boldsymbol{k}, \tag{10}$$

with

$$q = \begin{cases} \left(k_0^2 - \boldsymbol{k}^2\right)^{1/2} & \text{if } k_0^2 \geqslant \boldsymbol{k}^2 \\ \mathrm{j}\left(\boldsymbol{k}^2 - k_0^2\right)^{1/2} & \text{if } k_0^2 < \boldsymbol{k}^2 \end{cases} \qquad \text{and} \qquad \boldsymbol{R}_i = x_i\hat{\boldsymbol{x}} + y_i\hat{\boldsymbol{y}} + z_i\hat{\boldsymbol{z}} = \mathbf{r}_i + z_i\hat{\boldsymbol{z}}. \tag{10a}$$

In (10), instead of taking the absolute value $|z_2 - z_1|$ over the difference heights, Ishimaru *et al* [9] took it on the horizontal distance $|x_2 - x_1|$ whereas for Bahar's formulation [11], there is no term with absolute value. Ishimaru *et al* avoided to use $|z_2 - z_1|$ because the derivation of the ensemble average over $\{z_i\}$ is more complicated. Nevertheless, the use of $|x_2 - x_1|$ involves that the integrations over $\{x_i\}$ cannot be calculated analytically. In addition, the expansion over $|z_2 - z_1|$ is more relevant to obtain the geometric optics approximation for any random process.

To eliminate the absolute value over the height difference $z_2 - z_1$, the scattered field is split into wave positive and negative paths depicted in figure 4, and we have

$$G(\boldsymbol{R}_1, \boldsymbol{R}_2) = G_+(\boldsymbol{R}_1, \boldsymbol{R}_2) + G_-(\boldsymbol{R}_1, \boldsymbol{R}_2), \tag{11}$$

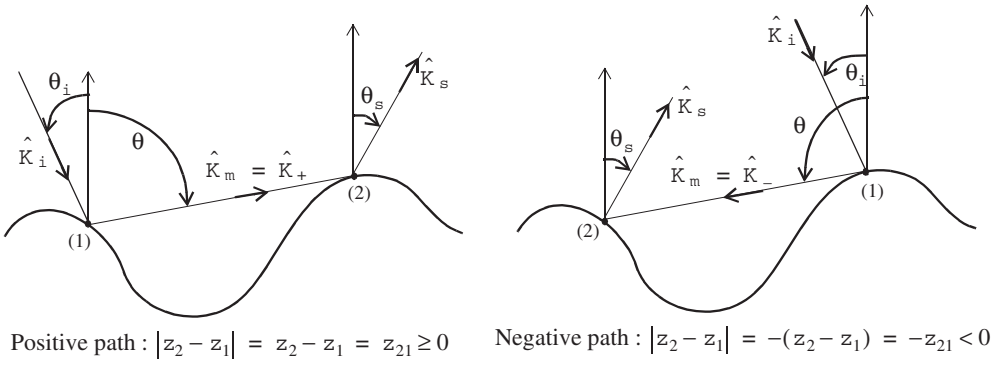


**Figure 4.** Illustration of the positive and negative paths of the scattered field.

where

$$G_m(\boldsymbol{R}_1, \boldsymbol{R}_2) = \frac{\mathrm{j}}{8\pi^2} \int \frac{1}{q} \exp\{\mathrm{j}[\boldsymbol{k} \cdot (\mathbf{r}_2 - \mathbf{r}_1) + mq(z_2 - z_1)]\} \, \mathrm{d}\boldsymbol{k}. \tag{11a}$$

For the sign plus ($m = +$), $z_2 \geqslant z_1$, whereas for the sign minus ($m = -$), $z_2 < z_1$. The substitution of (11) and (9) into (8) leads to

$$E_s^{i \to s} = \frac{\mathrm{j}(\mathrm{j}k_0)^2 E_0 \exp(\mathrm{j}k_0 R_0)}{4(2\pi)^3 R_0} (J_+ + J_-), \tag{12}$$

where

$$J_m = \int \bar{F}_m \, \Xi_{2m}(\mathbf{r}_1, \mathbf{r}_2) \exp\{\mathrm{j}[\boldsymbol{K}_i \cdot \boldsymbol{R}_1 - \boldsymbol{K}_s \cdot \boldsymbol{R}_2 + \boldsymbol{k} \cdot (\mathbf{r}_2 - \mathbf{r}_1) + mq(z_2 - z_1)]\} \, \mathrm{d}\boldsymbol{k} \, \mathrm{d}\mathbf{r}_1 \, \mathrm{d}\mathbf{r}_2. \tag{12a}$$

In (12$a$), $\Xi_{2m}(\mathbf{r}_1, \mathbf{r}_2)$ represents the second-order illumination function. $\Xi_{2m} = 1$ if a ray with a direction $\hat{\boldsymbol{K}}_i$ is not intercepted by the surface and strikes the point corresponding to $\mathbf{r}_1$, if the line drawn from the point $\mathbf{r}_1$ in the direction $\hat{\boldsymbol{K}}_m$ intercepts the surface at the point referred to as $\mathbf{r}_2$ and if the ray emanating from $\mathbf{r}_2$ in the direction $\hat{\boldsymbol{K}}_s$ does not cross the surface. Otherwise, $\Xi_{2m} = 0$.

The use of the stationary phase approximation implies that $\partial\Phi/\partial\mathbf{r}_i = 0$, where $\Phi$ denotes the argument of the exponential in (12$a$). This means that

$$\begin{cases} \dfrac{\partial \Phi}{\partial \mathbf{r}_1} = 0 \Rightarrow \boldsymbol{k}_i - \boldsymbol{k} + (q_i - mq)\dfrac{\partial z_1}{\partial \mathbf{r}_1} = 0 \Rightarrow \dfrac{\partial z_1}{\partial \mathbf{r}_1} = -\dfrac{\boldsymbol{k} - \boldsymbol{k}_i}{mq - q_i} \\ \dfrac{\partial \Phi}{\partial \mathbf{r}_2} = 0 \Rightarrow \boldsymbol{k} - \boldsymbol{k}_s + (mq - q_s)\dfrac{\partial z_2}{\partial \mathbf{r}_2} = 0 \Rightarrow \dfrac{\partial z_2}{\partial \mathbf{r}_2} = -\dfrac{\boldsymbol{k}_s - \boldsymbol{k}}{q_s - mq}, \end{cases} \tag{12b}$$

where $\boldsymbol{K}_{i,s} = \boldsymbol{k}_{i,s} + q_{i,s}\hat{\boldsymbol{z}}$. The normals to the surface at $\mathbf{r}_1$ and $\mathbf{r}_2$ then become

$$\hat{\boldsymbol{N}}_1 = \hat{\boldsymbol{N}}_{10} = (\boldsymbol{K}_m - \boldsymbol{K}_i)/\|\boldsymbol{K}_m - \boldsymbol{K}_i\| \qquad \text{and}$$
$$\hat{\boldsymbol{N}}_2 = \hat{\boldsymbol{N}}_{20} = (\boldsymbol{K}_s - \boldsymbol{K}_{-m})/\|\boldsymbol{K}_s - \boldsymbol{K}_{-m}\|. \tag{13}$$

Comparing (3) with (13), we can see that the stationary phase approximation of first order can be used before iteration to obtain the second-order stationary phase approximation. Thus, substituting (13) into (8$a$), the resulting equation is $\bar{F}_m = \bar{F}_{1m}$, where

$$\bar{F}_{1m}(\hat{\boldsymbol{K}}_i, \hat{\boldsymbol{K}}_m, \hat{\boldsymbol{K}}_s) = \bar{F}_1(\hat{\boldsymbol{K}}_i, \hat{\boldsymbol{K}}_m) \times \bar{F}_1(\boldsymbol{K}_{-m}, \hat{\boldsymbol{K}}_s)$$
$$= \begin{bmatrix} F_1^{v_i v_m} F_1^{v_{-m} v_s} + F_1^{v_i h_m} F_1^{h_{-m} v_s} & F_1^{v_i v_m} F_1^{v_{-m} h_s} + F_1^{v_i h_m} F_1^{h_{-m} h_s} \\ F_1^{h_i v_m} F_1^{v_{-m} v_s} + F_1^{h_i h_m} F_1^{h_{-m} v_s} & F_1^{h_i v_m} F_1^{v_{-m} h_s} + F_1^{h_i h_m} F_1^{h_{-m} h_s} \end{bmatrix}. \tag{14}$$

In the above equation, $\bar{F}_1(\hat{\boldsymbol{K}}_i, \hat{\boldsymbol{K}}_m)$ is given by (A2) where $\hat{\boldsymbol{K}}_s$ is substituted by $\hat{\boldsymbol{K}}_m$, which is similar to replace $\{\theta_s, \varphi_s\}$ by $\{\theta, \varphi\}$ for $m = +$ and by $\{\pi - \theta, \varphi\}$ for $m = -$. $\bar{F}_1(\boldsymbol{K}_{-m}, \hat{\boldsymbol{K}}_s)$ is given by (A2) where $\hat{\boldsymbol{K}}_i$ is substituted by $\boldsymbol{K}_{-m}$, which is similar to replace $\{\theta_i, \varphi_i\}$ by $\{\pi - \theta, \varphi\}$ for $m = +$ and by $\{\theta, \varphi\}$ for $m = -$. It must be noted that $\bar{F}_{1m}(\hat{\boldsymbol{K}}_i, \hat{\boldsymbol{K}}_m, \hat{\boldsymbol{K}}_s)$ obeys $\bar{F}_{1+}(\hat{\boldsymbol{K}}_i, \hat{\boldsymbol{K}}_+, \hat{\boldsymbol{K}}_s) = \bar{F}_{1-}(\hat{\boldsymbol{K}}_s, \hat{\boldsymbol{K}}_-, \hat{\boldsymbol{K}}_i)$ which ensures reciprocity.

### *2.3. Average scattered power*

This subsection presents the average scattered power obtained from the first- and second-order Kirchhoff approximations given by (6), (12) and denoted as $E_1$ and $E_2$, respectively. The superscript $i \to s$ which characterizes the polarization is omitted to facilitate the notation.

The total field $E_t$ is defined as

$$E_t = E_1 + E_2. \tag{15}$$

The average scattered power is expressed as

$$\langle E_t E_t'^* \rangle = \langle E_1 E_1'^* \rangle + 2\Re\langle E_2 E_1'^* \rangle + \langle E_2 E_2'^* \rangle, \tag{16}$$

where $\Re$ is the real part operator and * is the symbol for complex conjugate. To obtain the incoherent power $P_t$, we have to subtract the mean-square power from the total power. That is,

$$P_t = P_1 + P_{12} + P_2, \tag{17}$$

with

$$P_1 = \langle E_1 E_1'^* \rangle - |\langle E_1 \rangle|^2 = |k_0 E_0 \bar{F}_1(\hat{\boldsymbol{K}}_i, \hat{\boldsymbol{K}}_s)/(4\pi R_0)|^2 A_1, \tag{18}$$

$$\begin{aligned} P_{12} &= 2\Re[\langle E_2 E_1'^* \rangle - \langle E_2 \rangle \langle E_1'^* \rangle] \\ &= \frac{|E_0|^2 k_0^3}{4(2\pi)^4 R_0^2} \Re\left( \bar{F}_1^*(\hat{\boldsymbol{K}}_i, \hat{\boldsymbol{K}}_s) \int \frac{\bar{F}_{1m}(\hat{\boldsymbol{K}}_i, \hat{\boldsymbol{K}}_m, \hat{\boldsymbol{K}}_s) A_{12}}{q} \, \mathrm{d}\boldsymbol{k} \right), \end{aligned} \tag{19}$$

$$\begin{aligned} P_2 &= \langle E_2 E_2'^* \rangle - |\langle E_2 \rangle|^2 \\ &= \frac{|E_0|^2 k_0^4}{16(2\pi)^6 R_0^2} \int \frac{\bar{F}_{1m}(\hat{\boldsymbol{K}}_i, \hat{\boldsymbol{K}}_m, \hat{\boldsymbol{K}}_s) \bar{F}_{1m}(\hat{\boldsymbol{K}}_i, \hat{\boldsymbol{K}}_m', \hat{\boldsymbol{K}}_s)^* A_2}{q q'} \, \mathrm{d}\boldsymbol{k} \, \mathrm{d}\boldsymbol{k}', \end{aligned} \tag{20}$$

where

$$\begin{aligned} A_1 = \int \langle \Xi_1(\mathbf{r}_1) \Xi_1(\mathbf{r}_2) \exp[-\mathrm{j}(\boldsymbol{K}_s - \boldsymbol{K}_i) \cdot (\boldsymbol{R}_1 - \boldsymbol{R}_2)] \rangle \, \mathrm{d}\mathbf{r}_1 \, \mathrm{d}\mathbf{r}_2 \\ - \left| \int \langle \Xi_1(\mathbf{r}_1) \exp[-\mathrm{j}(\boldsymbol{K}_s - \boldsymbol{K}_i) \cdot \boldsymbol{R}_1] \rangle \, \mathrm{d}\mathbf{r}_1 \right|^2, \end{aligned} \tag{20a}$$

$$\begin{aligned} A_{12} = \int \{ \langle \Xi_{2m}(\mathbf{r}_1, \mathbf{r}_2) \Xi_1(\mathbf{r}_3) \exp\{ \mathrm{j}[\mathbf{K}_i \cdot (\boldsymbol{R}_1 - \boldsymbol{R}_3) + \boldsymbol{K}_s \cdot (\boldsymbol{R}_3 - \boldsymbol{R}_2) + \boldsymbol{k} \cdot (\mathbf{r}_2 - \mathbf{r}_1) \\ + mq(z_2 - z_1)] \} \rangle - \langle \exp\{ \mathrm{j}[\boldsymbol{K}_i \cdot \boldsymbol{R}_1 - \boldsymbol{K}_s \cdot \boldsymbol{R}_2 + \boldsymbol{k} \cdot (\mathbf{r}_2 - \mathbf{r}_1) \\ + mq(z_2 - z_1)] \} \rangle \langle \exp[\, \mathrm{j}(\boldsymbol{K}_s - \boldsymbol{K}_i) \cdot \boldsymbol{R}_3] \rangle \} \, \mathrm{d}\mathbf{r}_1 \, \mathrm{d}\mathbf{r}_2 \, \mathrm{d}\mathbf{r}_3, \end{aligned} \tag{20b}$$

$$\begin{aligned} A_2 = \int \langle \Xi_{2m}(\mathbf{r}_1, \mathbf{r}_2) \Xi_{2m}(\mathbf{r}_3, \mathbf{r}_4) \exp\{ \mathrm{j}[\boldsymbol{K}_i \cdot (\boldsymbol{R}_1 - \boldsymbol{R}_3) + \boldsymbol{K}_s \cdot (\boldsymbol{R}_4 - \boldsymbol{R}_2) + \boldsymbol{k} \cdot (\mathbf{r}_2 - \mathbf{r}_1) \\ + mq(z_2 - z_1) - \boldsymbol{k}' \cdot (\mathbf{r}_4 - \mathbf{r}_3) - m'q'(z_4 - z_3)] \} \rangle \, \mathrm{d}\mathbf{r}_1 \, \mathrm{d}\mathbf{r}_2 \, \mathrm{d}\mathbf{r}_3 \, \mathrm{d}\mathbf{r}_4 \\ - \left| \int \langle \Xi_{2m}(\mathbf{r}_1, \mathbf{r}_2) \exp\{ \mathrm{j}[\boldsymbol{K}_i \cdot \boldsymbol{R}_1 - \boldsymbol{K}_s \cdot \boldsymbol{R}_2 + \boldsymbol{k} \cdot (\mathbf{r}_2 - \mathbf{r}_1) \right. \\ \left. + mq(z_2 - z_1)] \} \rangle \, \mathrm{d}\mathbf{r}_1 \, \mathrm{d}\mathbf{r}_2 \right|^2. \end{aligned} \tag{20c}$$

The symbol $\langle\cdots\rangle$ denotes the ensemble average calculated over the surface elevations $\{z_i\}$. The incoherent scattering intensity is obtained by the multiplication of the scattered field with its complex conjugate from the field expression. To distinguish the conjugate from the field expression, the point (1) becomes (2) in (20*a*); in (20*c*) the points (1)–(2) become (3)–(4) and the vector $\boldsymbol{k}$ is denoted as $\boldsymbol{k}'$. In (15), when the second-order scattered field $E_2$ is added, the mean scattered power is defined as the sum of three incoherent scattered powers.

The random variables that appear in (20*a*)–(20*c*) are $z_i = z(\mathbf{r}_i)$, $\Xi_1(\mathbf{r}_i)$, $\Xi_{2m}(\mathbf{r}_i, \mathbf{r}_{i+1})$, respectively. In order to calculate the expected value, the shadowing effect is assumed to be statistically independent of the elevations $\{z_i\}$, which means that $p(\{z_i\}, \{\Xi_1\}, \{\Xi_{2m}\}) = p(\{z_i\}) \times p(\{\Xi_1\}, \{\Xi_{2m}\})$ where $p$ is the joint probability of the random variables. The ensemble average is then equal to the product of two ensemble averages $\langle\cdots\rangle = \langle\cdots\rangle_{\{z_i\}} \times \langle\cdots\rangle_{\{\Xi_1, \Xi_{2m}\}}$ obtained from the density functions $p(\{z_i\})$ and $p(\{\Xi_1\}, \{\Xi_{2m}\})$. For a Gaussian process, $\langle\cdots\rangle_{\{z_i\}}$ can be calculated analytically. For a stationary surface where the statistical properties depend only on the difference $\mathbf{r}_i - \mathbf{r}_j$, the total power $P_t$ therefore requires two-, six- and ten-fold integrations for the first-order, cross and second-order Kirchhoff terms $\{P_1, P_{12}, P_2\}$, respectively. To obtain an expression of the total incoherent scattered power usable numerically, additional assumptions such as the geometric optics approximation are then used.

Ishimaru's approach used the geometric optics approximation, which means that the correlations of $z_1 - z_2$ and $z_3 - z_4$ are very strong. The correlation between the elevation pair $\{z_1, z_2\}$ and $\{z_3, z_4\}$ is also neglected. It must also be noted that Ishimaru and Bahar implicitly assumed that the shadowing effect is statistically independent of the elevations $\{z_i\}$, and that the contribution of the cross term $P_{12}$ is omitted. Moreover, the probability density function is assumed to be Gaussian.

## 3. Incoherent scattering coefficient in the high-frequency limit

The geometric optics approximation (which is valid if the product $k_0\sigma_h$ is much larger than unity, with $k_0$ being the wave number, and $\sigma_h$ being the surface height rms) assumes that the scattering intensity gives contribution only for correlated closely located points. This means that the dashed lines in figures 5 and 6 for scattering from adjacent points are assumed to be close to the solid lines compared to the surface correlation length.

To simplify the expression of the incoherent scattering power obtained from (17), the expected value over the surface elevation is not performed, and the height difference $z_i - z_j$ of closely located points is expanded as $\boldsymbol{s}_j \cdot (\mathbf{r}_i - \mathbf{r}_j)$ where $\boldsymbol{s}_j = \partial z_j/\partial \mathbf{r}_j = s_{jx}\hat{\boldsymbol{x}} + s_{jy}\hat{\boldsymbol{y}}$ and $\{s_{jx}, s_{jy}\}$ are the surface slopes along the $\{\hat{\boldsymbol{x}}, \hat{\boldsymbol{y}}\}$ directions at the point $(j)$. In addition, the coherent contributions corresponding to the second terms of the right-hand sides of (20*a*)–(20*c*) can be omitted.

For any random process, we now derive the incoherent scattering coefficient $\sigma_i$ for first order (subscript $i = 1$), cross (subscript $i = 12$) and second order ($i = 2$). It is defined for a two-dimensional extended target as

$$\sigma_i = 4\pi R_0^2 P_i/(S_0|E_0|^2), \tag{21}$$

where $S_0 = (2L_{sx})(2L_{sy})$ is the illumination surface. $\{2L_{sx}, 2L_{sy}\}$ are the lengths of the foot print according to the $\{\hat{\boldsymbol{x}}, \hat{\boldsymbol{y}}\}$ directions, which are assumed to be much greater than the surface correlation lengths $\{L_{cx}, L_{cy}\}$ defined along the $\{\hat{\boldsymbol{x}}, \hat{\boldsymbol{y}}\}$ directions.

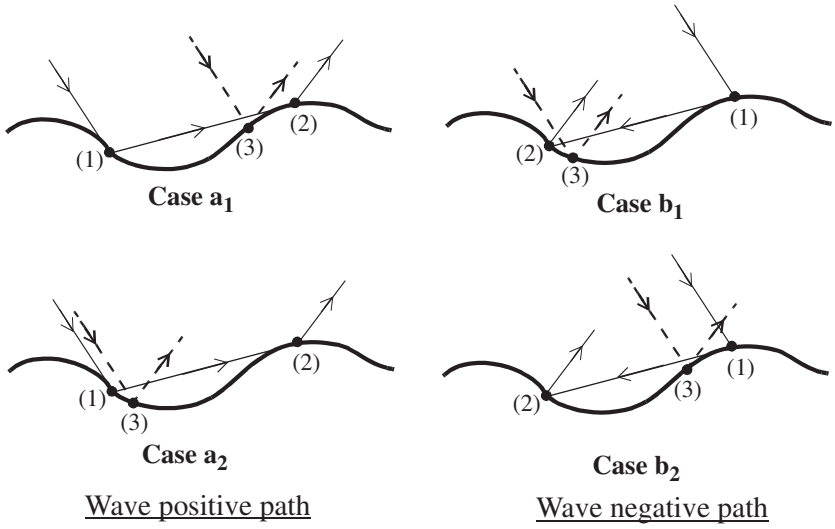


**Figure 5.** Geometrical representation of the incoherent term for the cross scattered power $P_{12}$. On the left, cases $\{a_{1,2}\}$ (point (3) close to the point (2) or (1)) exhibit the wave positive path. On the right, cases $\{b_{1,2}\}$ (point (3) close to the point (1) or (2)) display the wave negative path.

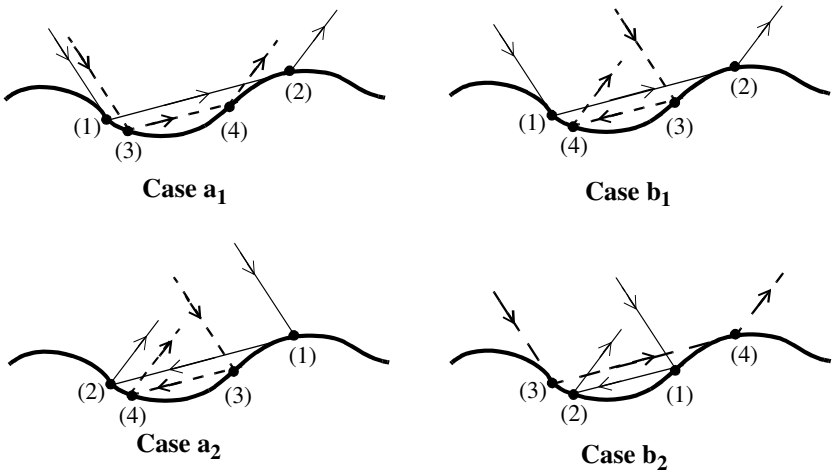


**Figure 6.** Geometrical representation of the incoherent term for (20*c*) ensemble average $A_2$. On the left, cases $\{a_{1,2}\}$ correspond to the ladder term exhibiting the double reflections from coincidental waves. On the right, cases $\{b_{1,2}\}$ denote the cross term showing the double reflections from anticoincidental waves.

### *3.1. First-order incoherent scattering*

In the high-frequency limit, since $z_2$ is close to $z_1$, $z_2 - z_1$ can be expanded as $\boldsymbol{s}_1 \cdot (\mathbf{r}_2 - \mathbf{r}_1)$. Thus, substituting (18) and (20*a*) into (21) by neglecting the coherent term and assuming a stationary surface, we get

$$\sigma_1 = \frac{|k_0 \bar{F}_1(\hat{\boldsymbol{K}}_i, \hat{\boldsymbol{K}}_s)|^2}{4\pi} \int_{S_0} \mathrm{d}\mathbf{r}_{21} \langle \Xi_1(\mathbf{r}_{21}) \exp\{\mathrm{j}[\boldsymbol{k}_s - \boldsymbol{k}_i + \boldsymbol{s}_1(q_s - q_i)] \cdot \mathbf{r}_{21}\} \rangle, \tag{22}$$

where the variable transformations $\mathbf{r}_{21} = \mathbf{r}_2 - \mathbf{r}_1$ and $\mathbf{r}_p = \mathbf{r}_2 + \mathbf{r}_1$ were used. The random variables which appear in the above equation are $\{\Xi_1, \boldsymbol{s}_1\}$. It is convenient to represent the density function $p(\boldsymbol{s}_1, \Xi_1)$ in terms of the conditional probability as [16]

$$p(\boldsymbol{s}_1, \Xi_1) = p_s(\boldsymbol{s}_1) \times p(\Xi_1|\boldsymbol{s}_1), \tag{23}$$

where $p_s(\boldsymbol{s}_1)$ is the slope joint distribution. This is the case because

$$p(\boldsymbol{s}_1, \Xi_1) = S_1(\hat{\boldsymbol{K}}_i, \hat{\boldsymbol{K}}_s|\boldsymbol{s}_1)\delta(\Xi_1 - 1) + [1 - S_1(\hat{\boldsymbol{K}}_i, \hat{\boldsymbol{K}}_s|\boldsymbol{s}_1)]\delta(\Xi_1), \tag{24}$$

where $\delta$ is the Dirac distribution. $S_1(\hat{\boldsymbol{K}}_i, \hat{\boldsymbol{K}}_s|\boldsymbol{s}_1)$ is the joint probability that a point on the surface will be illuminated by two rays having the directions $\{\hat{\boldsymbol{K}}_i, \hat{\boldsymbol{K}}_s\}$ with the knowledge of the slope $\boldsymbol{s}_1$. This function will be presented in subsection 4.1.

The contribution of the integrand is significant for $\{\mathbf{r}_{21} \cdot \hat{\boldsymbol{x}}, \mathbf{r}_{21} \cdot \hat{\boldsymbol{y}}\}$ smaller than $\{L_{cx}, L_{cy}\}$, where $\{L_{cx}, L_{cy}\}$ stand for the correlation lengths along the directions $\{\hat{\boldsymbol{x}}, \hat{\boldsymbol{y}}\}$. Moreover, the lengths $\{2L_{sx}, 2L_{sy}\}$ of the illuminated surface are assumed to be much greater than $\{L_{cx}, L_{cy}\}$, which allows us to transform the integration limit over $\mathbf{r}_{21}$ as $\{-\infty, \infty\}$. The integration over $\mathbf{r}_{21}$ of (22) then leads to

$$\sigma_1 = \pi|k_0\bar{F}_1(\hat{\boldsymbol{K}}_i, \hat{\boldsymbol{K}}_s)|^2\langle S_1(\hat{\boldsymbol{K}}_i, \hat{\boldsymbol{K}}_s|\boldsymbol{s}_1)\delta[\boldsymbol{k}_s - \boldsymbol{k}_i + \boldsymbol{s}_1(q_s - q_i)]\rangle. \tag{25}$$

Now the random variable is $\boldsymbol{s}_1$, and we have

$$\sigma_1 = \frac{\pi|k_0\bar{F}_1(\hat{\boldsymbol{K}}_i, \hat{\boldsymbol{K}}_s)|^2}{(q_s - q_i)^2} p_s\big(\boldsymbol{s}_1^0\big) S_1\big(\hat{\boldsymbol{K}}_i, \hat{\boldsymbol{K}}_s\big|\boldsymbol{s}_1^0\big), \tag{26}$$

where

$$\boldsymbol{s}_1^0 = -(\boldsymbol{k}_s - \boldsymbol{k}_i)/(q_s - q_i). \tag{26a}$$

This result has already been established by Sancer [16]. In what follows, the approach is extended to the second-order scattering.

### *3.2. Cross incoherent scattering coefficient*

In what follows, the formulation is not restricted to a Gaussian random process, unlike the formulations given by Ishimaru and Bahar. Indeed, the correlation between the random variables is described with the help of the covariance matrix, which involves that the mathematical expression of the density function is not required.

As seen in figure 5, the cases $\{a_1, a_2\}$ exhibit the wave positive paths referred to as $z_{21} \geqslant 0$ ($m = +$ in (20*b*)), whereas the cases $\{b_1, b_2\}$ display the wave negative paths corresponding to $z_{21} < 0$ ($m = -$ in (20*b*)).

For the contribution of the cases $\{a_1, b_1\}$, we use the following variable transformations:

$$\boldsymbol{R}_{21} = \boldsymbol{R}_2 - \boldsymbol{R}_1 \quad \text{and} \quad \boldsymbol{R}_{32} = \boldsymbol{R}_3 - \boldsymbol{R}_2. \tag{27}$$

In (20*b*), the exponential function with respect to $\{\mathbf{r}_i\}(\boldsymbol{K}_{i,s} = \boldsymbol{k}_{i,s} + q_{i,s}\hat{\boldsymbol{z}}$ and $\boldsymbol{R}_i = \mathbf{r}_i + z_i\hat{\boldsymbol{z}})$ of the incoherent term takes the form

$$\begin{aligned}&\exp\{\mathrm{j}[\boldsymbol{k}_i \cdot (\mathbf{r}_1 - \mathbf{r}_3) + \boldsymbol{k}_s \cdot (\mathbf{r}_3 - \mathbf{r}_2) + \boldsymbol{k} \cdot (\mathbf{r}_2 - \mathbf{r}_1) + mq(z_2 - z_1)]\}\\ &\qquad = \exp\{\mathrm{j}[(\boldsymbol{k}_s - \boldsymbol{k}_i) \cdot \mathbf{r}_{32} + (\boldsymbol{k} - \boldsymbol{k}_i) \cdot \mathbf{r}_{21}]\},\end{aligned} \tag{28}$$

and the ensemble average giving the contribution of the incoherent term is

$$\Theta_{12,I} = \langle \Xi_{2m}(\mathbf{r}_1, \mathbf{r}_2)\Xi_1(\mathbf{r}_3)\exp\{\mathrm{j}[z_{32}(q_s - q_i) + z_{21}(mq - q_i)]\}\rangle. \tag{29}$$

For the cases $\{a_1, b_1\}$, the point (2) is close to the point (3), which allows us to expand the height difference $z_{32}$ as $\boldsymbol{s}_2 \cdot \mathbf{r}_{32}$. Thus, substituting (19) and (20*b*) into (21) and using (28) and (29), the cross incoherent scattering coefficient for a stationary surface takes the form

$$\sigma_{12} = \frac{k_0^3}{2(2\pi)^3} \Re\left( \bar{F}_1^*(\hat{\boldsymbol{K}}_i, \hat{\boldsymbol{K}}_s) \int \frac{\bar{F}_{1m}(\hat{\boldsymbol{K}}_i, \hat{\boldsymbol{K}}_m, \hat{\boldsymbol{K}}_s) A_{12}}{q} \, \mathrm{d}\boldsymbol{k} \right), \tag{30}$$

where

$$A_{12} = \int_{S_0} \mathrm{d}\mathbf{r}_{21} \, \mathrm{d}\mathbf{r}_{32} \langle \Xi_{2m}(\mathbf{r}_1, \mathbf{r}_2) \Xi_1(\mathbf{r}_3) \exp\{ \mathrm{j}[\boldsymbol{k}_s - \boldsymbol{k}_i + \boldsymbol{s}_2(q_s - q_i)] \cdot \mathbf{r}_{32} + j(\boldsymbol{k} - \boldsymbol{k}_i) \cdot \mathbf{r}_{21} + j z_{21}(mq - q_i) \} \rangle. \tag{30a}$$

It must noted that the integration over $\mathbf{r}_3$, where $\mathrm{d}\mathbf{r}_1 \, \mathrm{d}\mathbf{r}_2 \, \mathrm{d}\mathbf{r}_3 = \mathrm{d}\mathbf{r}_{21} \, \mathrm{d}\mathbf{r}_{32} \, \mathrm{d}\mathbf{r}_3$, gives $S_0 \, \mathrm{d}\mathbf{r}_{21} \, \mathrm{d}\mathbf{r}_{32}$ where $S_0$ is the illuminated foot print. To simplify $\sigma_{12}$, we used the following three assumptions: (i) the correlation between the points (1) and (2) is omitted; (ii) to be consistent with the geometric optics approximation, the evanescent waves are neglected. See appendix D for more details; (iii) to quantify the fact that the scattered waves at the point (1) propagate only in certain distance before being intercepted by the surface at the point (2), a tapering function $\chi_t$ defined as (B9) is included in $\sigma_{12}$. The resulting equation is then (see appendix B)

$$\sigma_{12} = \frac{\pi k_0^2 p_s\left(\boldsymbol{s}_2^0\right)}{4(q_s - q_i)^2} \Re\left\{ \bar{F}_1^*(\hat{\boldsymbol{K}}_i, \hat{\boldsymbol{K}}_s) \int_0^{\pi/2} \sin\theta \, \mathrm{d}\theta \int_0^{2\pi} \bar{F}_{1m}(\hat{\boldsymbol{K}}_i, \hat{\boldsymbol{K}}_m, \hat{\boldsymbol{K}}_s) \chi_t(\boldsymbol{k} - \boldsymbol{k}_i) \times \left\langle S_{12}\left(\hat{\boldsymbol{K}}_i, \hat{\boldsymbol{K}}_s, \hat{\boldsymbol{K}}_m \middle| \boldsymbol{s}_2^0, z_{21}\right) \exp[\, \mathrm{j} z_{21}(mq - q_i)] \right\rangle \mathrm{d}\varphi \right\}. \tag{31}$$

For the contribution of the cases $\{a_2, b_2\}$, the following variable transformations are used:

$$\boldsymbol{R}_{21} = \boldsymbol{R}_2 - \boldsymbol{R}_1 \quad \text{and} \quad \boldsymbol{R}_{31} = \boldsymbol{R}_3 - \boldsymbol{R}_1. \tag{32}$$

Applying the same way, the incoherent scattering coefficient is then given by

$$\sigma_{12} = \text{equation (31) where } \hat{\boldsymbol{K}}_i \text{ is transposed by } \hat{\boldsymbol{K}}_s \text{ in the integrand.} \tag{33}$$

Therefore, since $\bar{F}_{1-}(\hat{\boldsymbol{K}}_i, \hat{\boldsymbol{K}}_-, \hat{\boldsymbol{K}}_s) = \bar{F}_{1+}(\hat{\boldsymbol{K}}_s, \hat{\boldsymbol{K}}_+, \hat{\boldsymbol{K}}_i)$ the reciprocity is ensured.

### *3.3. Second-order scattering coefficient*

In (20*c*), the splitting up of the ensemble average $\Theta_{2,I}$ into positive and negative paths leads to

$$\Theta_{2,I} = \langle (I_+ F_{1+} + I_- F_{1-})(I_+ F_{1+} + I_- F_{1-})'^* \rangle = F_{1+} F_{1+}'^* \langle I_+ I_+'^* \rangle + F_{1-} F_{1-}'^* \langle I_- I_-'^* \rangle + 2\Re(F_{1+} F_{1-}'^* \langle I_+ I_-'^* \rangle), \tag{34}$$

where

$$\langle I_+ I_+'^* \rangle = \langle \Xi_{2+} \Xi_{2+}' \exp\{ \mathrm{j}[q_i z_{13} - q_s z_{24} + q z_{21} - q' z_{43}] \} \rangle, \quad \text{for} \quad \{z_{21} \geqslant 0, z_{43} \geqslant 0\} \quad \text{and} \quad \{m = +, m' = +\}, \tag{34a}$$

$$\langle I_- I_-'^* \rangle = \langle \Xi_{2-} \Xi_{2-}' \exp\{ \mathrm{j}[q_i z_{13} - q_s z_{24} - q z_{21} + q' z_{43}] \} \rangle \quad \text{for} \quad \{z_{21} < 0, z_{43} < 0\} \quad \text{and} \quad \{m = -, m' = -\}, \tag{34b}$$

$$\langle I_+ I_-'^* \rangle = \langle \Xi_{2+} \Xi_{2-}' \exp\{ \mathrm{j}[q_i z_{13} - q_s z_{24} + q z_{21} + q' z_{43}] \} \rangle \quad \text{for} \quad \{z_{21} \geqslant 0, z_{43} < 0\} \quad \text{and} \quad \{m = +, m' = -\}, \tag{34c}$$

where

$$z_{ij} = z_i - z_j,\ \Xi_{2m} = \Xi_{2m}(\mathbf{r}_1, \mathbf{r}_2),\ \Xi'_{2m} = \Xi_{2m}(\mathbf{r}_3, \mathbf{r}_4),\ F'_{1m} = F_{1m}(\hat{\boldsymbol{K}}_i, \hat{\boldsymbol{K}}_m, \hat{K}_s)\big|_{\hat{K}_m = \hat{K}'_m}. \tag{34d}$$

The ensemble average $\langle I_+ I'^*_+ \rangle + \langle I_- I'^*_- \rangle$ gives the contribution of the coincidental waves exhibited in figure 6 (cases $\{a_{1,2}\}$ where the wave paths are in the same direction, both either positive or negative), whereas $\langle I_+ I'^*_- \rangle$ gives the contribution of the anticoincidental waves shown in figure 6 (cases $\{b_{1,2}\}$ where the wave paths are in opposite directions).

*3.3.1. Contribution of the coincidental waves.* We use the following variable transformations of $\{\boldsymbol{R}_{1,2,3,4}\}$ into $\{\boldsymbol{R}_{31}, \boldsymbol{R}_{24}, \boldsymbol{R}_d\}$:

$$\begin{cases} \boldsymbol{R}_{31} = \boldsymbol{R}_3 - \boldsymbol{R}_1 \\ \boldsymbol{R}_{24} = \boldsymbol{R}_2 - \boldsymbol{R}_4 \\ \boldsymbol{R}_{p1} = (\boldsymbol{R}_1 + \boldsymbol{R}_3)/2 \\ \boldsymbol{R}_{p2} = (\boldsymbol{R}_2 + \boldsymbol{R}_4)/2 \end{cases} \Rightarrow \begin{cases} \boldsymbol{R}_1 = \boldsymbol{R}_{p1} - \boldsymbol{R}_{31}/2 \\ \boldsymbol{R}_3 = \boldsymbol{R}_{p1} + \boldsymbol{R}_{31}/2 \\ \boldsymbol{R}_2 = \boldsymbol{R}_{p2} + \boldsymbol{R}_{24}/2 \\ \boldsymbol{R}_4 = \boldsymbol{R}_{p2} - \boldsymbol{R}_{24}/2 \end{cases} \quad \text{and} \quad \boldsymbol{R}_d = \boldsymbol{R}_{p2} - \boldsymbol{R}_{p1}. \tag{35}$$

In (20*c*), the exponential function according to the components $\{\mathbf{r}_i\}$ is then

$$\exp\{\mathrm{j}[\boldsymbol{k}_i \cdot (\mathbf{r}_1 - \mathbf{r}_3) + \boldsymbol{k}_s \cdot (\mathbf{r}_4 - \mathbf{r}_2) + \boldsymbol{k} \cdot (\mathbf{r}_2 - \mathbf{r}_1) - \boldsymbol{k}' \cdot (\mathbf{r}_4 - \mathbf{r}_3)]\} = \exp\left\{\mathrm{j}\left[\left(\frac{\boldsymbol{k} + \boldsymbol{k}'}{2} - \boldsymbol{k}_i\right) \cdot \mathbf{r}_{31} + \left(\frac{\boldsymbol{k} + \boldsymbol{k}'}{2} - \boldsymbol{k}_s\right) \cdot \mathbf{r}_{24} + (\boldsymbol{k} - \boldsymbol{k}') \cdot \mathbf{r}_d\right]\right\}. \tag{36}$$

In addition, for $\langle I_\pm I'^*_\pm \rangle$, we have

$$\langle I_\pm I'^*_\pm \rangle = \left\langle \Xi_{2\pm} \Xi'_{2\pm} \exp\left\{\mathrm{j}\left[\left(\pm\frac{q + q'}{2} - q_i\right) z_{31} + \left(\pm\frac{q + q'}{2} - q_s\right) z_{24} \pm (q - q') z_d\right]\right\}\right\rangle. \tag{37}$$

For the cases $\{a_1, a_2\}$ in figure 6, the point (1) must be close to the point (3) and the point (2) must be close to the point (4). The height differences $z_{31} = z_3 - z_1$ and $z_{24} = z_2 - z_4$ can be then expanded as $\boldsymbol{s}_1 \cdot \mathbf{r}_{31}$ and $\boldsymbol{s}_2 \cdot \mathbf{r}_{24}$, respectively, where $\boldsymbol{s}_1 \approx \boldsymbol{s}_2$, for which $\{\boldsymbol{s}_1, \boldsymbol{s}_2\}$ are the surface slopes at the points (1) and (2). These equalities imply in (20) that $\hat{\boldsymbol{K}}_m \approx \hat{\boldsymbol{K}}'_m$ and $\bar{F}_{1m}(\hat{\boldsymbol{K}}_i, \hat{\boldsymbol{K}}_m, \hat{\boldsymbol{K}}_s) \bar{F}_{1m}(\hat{\boldsymbol{K}}_i, \hat{\boldsymbol{K}}'_m, \hat{\boldsymbol{K}}_s)^* \approx |\bar{F}_{1m}(\hat{\boldsymbol{K}}_i, \hat{\boldsymbol{K}}'_m, \hat{\boldsymbol{K}}_s)|^2$.

With $\boldsymbol{R}_{21} = \boldsymbol{R}_d - (\boldsymbol{R}_{24} + \boldsymbol{R}_{31})/2$, the above equations take the form

$$\text{Equation (36)} = \exp\{\mathrm{j}[(\boldsymbol{k}' - \boldsymbol{k}_i) \cdot \mathbf{r}_{31} + (\boldsymbol{k}' - \boldsymbol{k}_s) \cdot \mathbf{r}_{24} + (\boldsymbol{k} - \boldsymbol{k}') \cdot \mathbf{r}_{21}]\}, \tag{38}$$

and

$$\langle I_\pm I'^*_\pm \rangle = \langle \Xi_{2\pm} \Xi'_{2\pm} \exp\{\mathrm{j}[(\pm q' - q_i) \boldsymbol{s}_1 \cdot \mathbf{r}_{31} + (\pm q' - q_s) \boldsymbol{s}_2 \cdot \mathbf{r}_{24} \pm (q - q') z_{21}]\}\rangle. \tag{39}$$

The substitution of (20) into (21) yields the following incoherent scattering coefficient (subscript *c* for coincidental waves):

$$\sigma_{2c} = \frac{k_0^4}{8(2\pi)^5} \int \frac{|\bar{F}_{1m}(\hat{\boldsymbol{K}}_i, \hat{\boldsymbol{K}}'_m, \hat{\boldsymbol{K}}_s)|^2 A_2}{q q'} \, \mathrm{d}\boldsymbol{k} \, \mathrm{d}\boldsymbol{k}', \tag{40}$$

where

$$A_2 = \int_{s_0} \mathrm{d}\mathbf{r}_{21} \, \mathrm{d}\mathbf{r}_{31} \, \mathrm{d}\mathbf{r}_{24} \langle I_\pm I'^*_\pm \rangle \times \text{ equation (38)}. \tag{40a}$$

To simplify $\sigma_{2c}$, we used the following three assumptions; (i) the correlation between the points (1) and (2) and (3) and (4) is omitted; (ii) to be consistent with the geometric optics approximation, the evanescent waves are neglected—see appendix D for more details; (iii) to quantify the fact that the scattered waves at the point (1) propagate only in certain distance

before being intercepted by the surface at the point (2), a tapering function $\chi_t$ defined as (B9) is included in $\sigma_{2c}$. The resulting equation is then (see appendix C)

$$\sigma_{2c} = \frac{\pi k_0^4}{16}\int_0^{\pi/2}\mathrm{d}\theta\int_0^{\pi/2}\mathrm{d}\theta'\int_0^{2\pi}\mathrm{d}\varphi\int_0^{2\pi}\mathrm{d}\varphi'\frac{|\bar{F}_{1m}(\hat{\boldsymbol{K}}_i,\hat{\boldsymbol{K}}'_m,\hat{\boldsymbol{K}}_s)|^2\chi_t(\boldsymbol{k}-\boldsymbol{k}')\sin\theta\sin\theta'}{(\pm q'-q_i)^2(\pm q'-q_s)^2}$$
$$p_s\big(\boldsymbol{s}_1^{0c}\big)p_s\big(\boldsymbol{s}_2^{0c}\big)\big\langle S_c\big(\hat{\boldsymbol{K}}_i,\hat{\boldsymbol{K}}_m,\hat{\boldsymbol{K}}_s\big|\boldsymbol{s}_1^{0c},\boldsymbol{s}_2^{0c},z_{21}\big)\exp[\pm\mathrm{j}(q-q')z_{21}]\big\rangle, \tag{41}$$

where the slopes $\{\boldsymbol{s}_{1,2}^{0c}\}$ are given by (C5). For the derivation of the ensemble average, the only random variable is $z_{21}$ where $\langle z_{21}^2\rangle = 2\sigma_h^2$. The integrand is maximum, when $\hat{\boldsymbol{K}} = \hat{\boldsymbol{K}}'$.

*3.3.2. Contribution of the anticoincidental waves.* We use the following variable transformations of $\{\boldsymbol{R}_{1,2,3,4}\}$ into $\{\boldsymbol{R}_{41},\boldsymbol{R}_{23},\boldsymbol{R}_d\}$:

$$\begin{cases}\boldsymbol{R}_{41}=\boldsymbol{R}_4-\boldsymbol{R}_1\\ \boldsymbol{R}_{23}=\boldsymbol{R}_2-\boldsymbol{R}_3\\ \boldsymbol{R}_{p1}=(\boldsymbol{R}_1+\boldsymbol{R}_4)/2\\ \boldsymbol{R}_{p2}=(\boldsymbol{R}_2+\boldsymbol{R}_3)/2\end{cases}\Rightarrow\begin{cases}\boldsymbol{R}_1=\boldsymbol{R}_{p1}-\boldsymbol{R}_{41}/2\\ \boldsymbol{R}_4=\boldsymbol{R}_{p1}+\boldsymbol{R}_{41}/2\\ \boldsymbol{R}_2=\boldsymbol{R}_{p2}+\boldsymbol{R}_{23}/2\\ \boldsymbol{R}_3=\boldsymbol{R}_{p2}-\boldsymbol{R}_{23}/2\end{cases}\quad\text{and}\quad\boldsymbol{R}_d=\boldsymbol{R}_{p2}-\boldsymbol{R}_{p1.} \tag{42}$$

Therefore, using the same procedure as the coincidental waves, the incoherent scattering coefficient giving the contribution of the anticoincidental (subscript $a$) waves is

$$\sigma_{2a} = \frac{\pi k_0^4}{8}\Re\left\{\int_0^{\pi/2}\mathrm{d}\theta\int_0^{\pi/2}\mathrm{d}\theta'\int_0^{\pi/2}\mathrm{d}\varphi\int_0^{\pi/2}\mathrm{d}\varphi'\right.$$
$$\times\frac{|\bar{F}_{1-}(\hat{\boldsymbol{K}}_i,\hat{\boldsymbol{K}}'_-,\hat{\boldsymbol{K}}_s)^2|\sin\theta\sin\theta' p_s\big(\boldsymbol{s}_1^{0a}\big)p_s\big(\boldsymbol{s}_2^{0a}\big)}{(q'+q_s)^2(q'+q_i)^2}$$
$$\times\chi_t(\boldsymbol{k}+\boldsymbol{k}'-\boldsymbol{k}_i-\boldsymbol{k}_s)\big\langle S_a\big(\hat{\boldsymbol{K}}_i,\hat{\boldsymbol{K}}'_-,\hat{\boldsymbol{K}}_s\big|\boldsymbol{s}_1^{0a},\boldsymbol{s}_2^{0a},z_{21}\big)$$
$$\left.\times\exp[\,\mathrm{j}(q-q'-q_i-q_s)z_{21}]\big\rangle\right\}, \tag{43}$$

where

$$\boldsymbol{s}_1^{0a} = -(\boldsymbol{k}_s-\boldsymbol{k}')/(q_s+q'),\qquad \boldsymbol{s}_2^{0a} = -(\boldsymbol{k}_i-\boldsymbol{k}')/(q_i+q'). \tag{43a}$$

The major contributions come from the regions where $\hat{\boldsymbol{K}}_+ + \hat{\boldsymbol{K}}'_- - \hat{\boldsymbol{K}}_i - \hat{\boldsymbol{K}}_s \approx \boldsymbol{0}$. From figure 6, for the anticoincidental waves, we have $\hat{\boldsymbol{K}}'_- \approx -\hat{\boldsymbol{K}}_+$. The rays are then quasi-antiparallel and $\hat{\boldsymbol{K}}_s \approx -\hat{\boldsymbol{K}}_i$ occurring in the backscattering direction defined as $\{\theta_s = -\theta_i, \varphi_s = \varphi_i\}$, which gives in consequence the backscattering enhancement.

## 4. Shadowing function

Ishimaru and Bahar formulations and the IEM model derived the second-order illumination function from the average shadowing function with single reflection by using a geometrical way and by assuming an isotropic surface. Recently, for a 1D surface and for any uncorrelated process, Bourlier *et al* [12] calculated rigorously the second-order illumination function, which is expressed from the monostatic statistical shadowing function with single reflection. Moreover, they showed that the monostatic statistical shadowing function obtained from 1D surface can be extended to a 2D anisotropic surface [17, 18].

In this section, the shadowing effect with single and double reflections is presented and a procedure is given in order to include it in the first- and second-order incoherent scattering coefficients.

*4.1. Bistatic shadowing function with single reflection*

In this subsection, the first-order average bistatic shadowing function $S_1\big(\hat{\boldsymbol{K}}_i, \hat{\boldsymbol{K}}_s \big| \boldsymbol{s}_1^0\big)$, which appears in (26) for the derivation of $\sigma_1$, is determined. Unlike a 1D surface, for the calculation of the first-order illumination function of a 2D surface, three cases have to be considered $\varphi_s = \varphi_i$, $\varphi_s = \varphi_i + \pi$ and $\{\varphi_s \neq \varphi_i, \varphi_s \neq \varphi_i + \pi\}$ (transmitter and the receiver are in different planes).

When the transmitter and the receiver are located in the same plane, i.e. $\{\varphi_s = \varphi_i, \varphi_s = \varphi_i + \pi\}$, the issue is similar to a 1D surface since the surface slope viewed both by the transmitter and the receiver is the same.

From [18], for an infinite observation length with $\varphi_s = \varphi_i$, the bistatic statistical shadowing function is

$$S_b(\hat{\boldsymbol{K}}_i, \hat{\boldsymbol{K}}_s, z_0, s_{0X}) = \begin{cases} S(\hat{\boldsymbol{K}}_i, z_0, s_{0X}) S(\hat{\boldsymbol{K}}_s, z_0, s_{0X}) & \text{if } \theta_s \in [0; \pi/2] \\ S(\hat{\boldsymbol{K}}_i, z_0, s_{0X}) & \text{if } \theta_s \in [-\theta_i; 0[ \\ S(\hat{\boldsymbol{K}}_s, z_0, s_{0X}) & \text{if } \theta_s \in [-\pi/2; -\theta_i[ \end{cases} \quad \text{for } \varphi_s = \varphi_i. \tag{44}$$

The monostatic statistical shadowing function $S_m(\hat{\boldsymbol{K}}, z_0, s_{0X})$ is defined as

$$S(\hat{\boldsymbol{K}}, z_0, s_{0X}) = \Upsilon(\mu - s_{0X})[P_h(z_0) - P_h(-\infty)]^{\Lambda(\hat{\boldsymbol{K}})}, \tag{44a}$$

where

$$\Lambda(\hat{\boldsymbol{K}}) = \Lambda(\theta, \varphi) = \frac{1}{\mu} \int_{\mu}^{\infty} (s_{0X} - \mu) p_s(s_{0X}) \, \mathrm{d}s_{0X} \quad \text{and} \quad \mu = \cot\theta. \tag{44b}$$

In the above equations, $P_h$ stands for a primitive of the height distribution, $\Upsilon$ is the unit step function defined as $\Upsilon(x) = 1$ for $x \geqslant 0$ else 0, $s_{0X}$ is the surface slopes viewed by the incident ray of direction $\hat{\boldsymbol{K}}$ along the azimuthal angle $\varphi$ and $s_{0X} = s_{0x} \cos\varphi + s_{0y} \sin\varphi$, where $\{s_{0x}, s_{0y}\}$ are the surface slopes along the directions $\{\hat{\boldsymbol{x}}, \hat{\boldsymbol{y}}\}$. $p_s(s_{0X})$ stands for the marginal slope probability density function with

$$\text{mean value } \langle s_{0X} \rangle \text{ since } \langle s_{0x} \rangle = \langle s_{0y} \rangle = 0, \tag{45}$$

$$\text{variance } \big\langle s_{0X}^2 \big\rangle = \sigma_{sx}^2 (\cos\varphi)^2 + \sigma_{sy}^2 (\sin\varphi)^2 \text{ since } \big\langle s_{0x,0y}^2 \big\rangle = \sigma_{sx,sy}^2 \text{ and } \langle s_{0x} s_{0y} \rangle = 0. \tag{46}$$

$\big\{\sigma_{sx,sy}^2\big\}$ are the slope variances along the directions $\{\hat{\boldsymbol{x}}, \hat{\boldsymbol{y}}\}$. In [17], a method is addressed for the derivation of $p_s(s_{0X})$ knowing $p_s(s_{0x}, s_{0y})$.

In (44*a*), the shadowing effect modifies the height distribution at once, due to the $P_h$ function, and $\Upsilon(\mu - s_{0X})$ carries a restriction over the slopes $\gamma_{0X}$. From (44), this implies that $\{s_{0X} \in [-\mu_i; \mu_s], s_{0X} \in ]-\infty; \mu_i], s_{0X} \in ]-\infty; \mu_s]\}$ for each case. From figure 1, this leads to $|\theta_1| < \pi/2$. In (26), the knowledge of the slope $\boldsymbol{s}_1^0$, given by (26*a*), involves that $\cos\theta_1 = -\boldsymbol{N}_1 \cdot \hat{\boldsymbol{K}}_i = q_1/2$ where $q_1$ is expressed from (A6). Since $0 \leqslant q_1 < 2$, we have $0 \leqslant \cos\theta_1 < 1 \Rightarrow 0 \leqslant \theta_1 < \pi/2$, which means that $|\theta_1|$ is always strictly smaller than $\pi/2$. Therefore, there is no restriction over the surface slope and the only random variable in (44) is $z_0$. We have

$$S_1\big(\hat{\boldsymbol{K}}_i, \hat{\boldsymbol{K}}_s | \boldsymbol{s}_1^0\big) = \langle P_h(z_0) S_b(\hat{\boldsymbol{K}}_i, \hat{\boldsymbol{K}}_s, z_0) \rangle, \tag{47}$$

which leads for any process to

$$S_1\big(\hat{\boldsymbol{K}}_i, \hat{\boldsymbol{K}}_s \big| \boldsymbol{s}_1^0\big) = \begin{cases} [1 + \Lambda(\hat{\boldsymbol{K}}_i) + \Lambda(\hat{\boldsymbol{K}}_s)]^{-1} & \text{if } \theta_s \in [0; \pi/2] \\ [1 + \Lambda(\hat{\boldsymbol{K}}_i)]^{-1} & \text{if } \theta_s \in [-\theta_i; 0[ \\ [1 + \Lambda(\hat{\boldsymbol{K}}_s)]^{-1} & \text{if } \theta_s \in [-\pi/2; -\theta_i[ \end{cases} \quad \text{for } \varphi_s = \varphi_i. \tag{48}$$

Applying the same way for $\varphi_s = \varphi_i + \pi_i$, we obtain

$$S_1\big(\hat{\boldsymbol{K}}_i, \hat{\boldsymbol{K}}_s \big| \boldsymbol{s}_1^0\big) = \begin{cases} [1 + \Lambda(\hat{\boldsymbol{K}}_i) + \Lambda(\hat{\boldsymbol{K}}_s)]^{-1} & \text{if } \theta_s \in [-\pi/2; 0] \\ [1 + \Lambda(\hat{\boldsymbol{K}}_i)]^{-1} & \text{if } \theta_s \in ]0; \theta_i] \\ [1 + \Lambda(\hat{\boldsymbol{K}}_s)]^{-1} & \text{if } \theta_s \in ]\theta_i; \pi/2] \end{cases} \quad \text{for } \varphi_s = \varphi_i + \pi_i. \tag{49}$$

In the above equations, $\Lambda(\hat{\boldsymbol{K}})$ is defined as (44*b*) which depends on the marginal slope probability $p_s(s_{0X})$.

For $\{\varphi_s \neq \varphi_i, \varphi_s \neq \varphi_i + \pi\}$ (transmitter and receiver in different planes), the slopes $\big\{s_{0X_i}, s_{0X_s}\big\}$ observed by the emitter and the receiver are not equal and we have [18]

$$S_b\big(\hat{\boldsymbol{K}}_i, \hat{\boldsymbol{K}}_s, z_0, s_{0X_i}, s_{0X_s}\big) = \Upsilon\big(\mu_s - s_{0X_s}\big)\Upsilon\big(\mu_i + s_{0X_i}\big)[P_h(z_0) - P_h(-\infty)]^{\Lambda(\hat{\boldsymbol{K}}_i)+\Lambda(\hat{\boldsymbol{K}}_s)}. \tag{50}$$

As previously mentioned, the knowledge of $\boldsymbol{s}_1^0$ implies that there is no restriction over the surface slopes $\big\{s_{0X_i}, s_{0X_s}\big\}$ and the only random variable is then $z_0$. Averaging (50), the resulting equation is then

$$S_1\big(\hat{\boldsymbol{K}}_i, \hat{\boldsymbol{K}}_s \big| \boldsymbol{s}_1^0\big) = [1 + \Lambda(\hat{\boldsymbol{K}}_i) + \Lambda(\hat{\boldsymbol{K}}_s)]^{-1} \qquad \text{for} \quad \{\varphi_s \neq \varphi_i, \varphi_s \neq \varphi_i + \pi\}. \tag{51}$$

### *4.2. Bistatic shadowing function with double reflection*

This section is devoted to the calculations of the average shadowing functions that appear in (31), (41) and (43).

*4.2.1. Case of the cross incoherent scattering coefficient.* In (44*a*), we can observe that the shadow carries a restriction over the surface slopes through the Heaviside function $\Upsilon$. From figure 1, this leads to $|\theta_1| < \pi/2$. Hence, for a double reflection, as depicted in figure 3, we must get $\{\theta_1, \theta_2\} \in \{]-\pi/2; \pi/2[\}$ depending on $\{\theta_i, \theta_s, \theta\}$, since the slopes at these points are performed from the stationary phase method. In (31), for the derivation of $\sigma_{12}$, $S_{12}\big(\hat{\boldsymbol{K}}_i, \hat{\boldsymbol{K}}_s, \hat{\boldsymbol{K}}_m \big| \boldsymbol{s}_2^0, z_{21}\big)$ has to be performed. In $S_{12}$, the knowledge of $\boldsymbol{s}_2^0$ given by (B7) involves that $\theta = \pi - \theta_i$ and the slope at the point (1) are given by (26*a*) where $\boldsymbol{s}_1^0 = \boldsymbol{s}_2^0$, which means that $\theta = \theta_s$. In addition, from figure 3, we have $\theta_1 = (\theta + \theta_i)/2$ and $\theta_2 = (\pi + \theta_s - \theta)/2$ which means that $\theta_1 = \theta_2 = \pi/2$. Thus, the slopes at the points (1) and (2) are hidden and the contribution of the cross incoherent scattering coefficient $\sigma_{12}$ is equal to zero due to the shadow. In [9], this term is neglected without justification.

*4.2.2. Second-order bistatic statistical shadowing function.* From [12], we have for a 2D surface

$$S_{2+}(\hat{\boldsymbol{K}}_i, \hat{\boldsymbol{K}}_+, \hat{\boldsymbol{K}}_s, F_1, F_2) = \begin{cases} S(\hat{\boldsymbol{K}}_i, \infty, F_1)\tilde{S}(\hat{\boldsymbol{K}}_+, l_2, F_1)S(\hat{\boldsymbol{K}}_s, \infty, F_2) & \text{Case } (b_{1+}) \\ 0 & \text{Case } (b_{2+}) \\ S(\hat{\boldsymbol{K}}_i, \infty, F_1)\tilde{S}(\hat{\boldsymbol{K}}_+, l_2, F_1) & \text{Case } (b_{3+}) \\ S(\hat{\boldsymbol{K}}_s, \infty, F_1)\tilde{S}(\hat{\boldsymbol{K}}_+, l_2, F_1) & \text{Case } (b_{4+}), \end{cases} \tag{52}$$

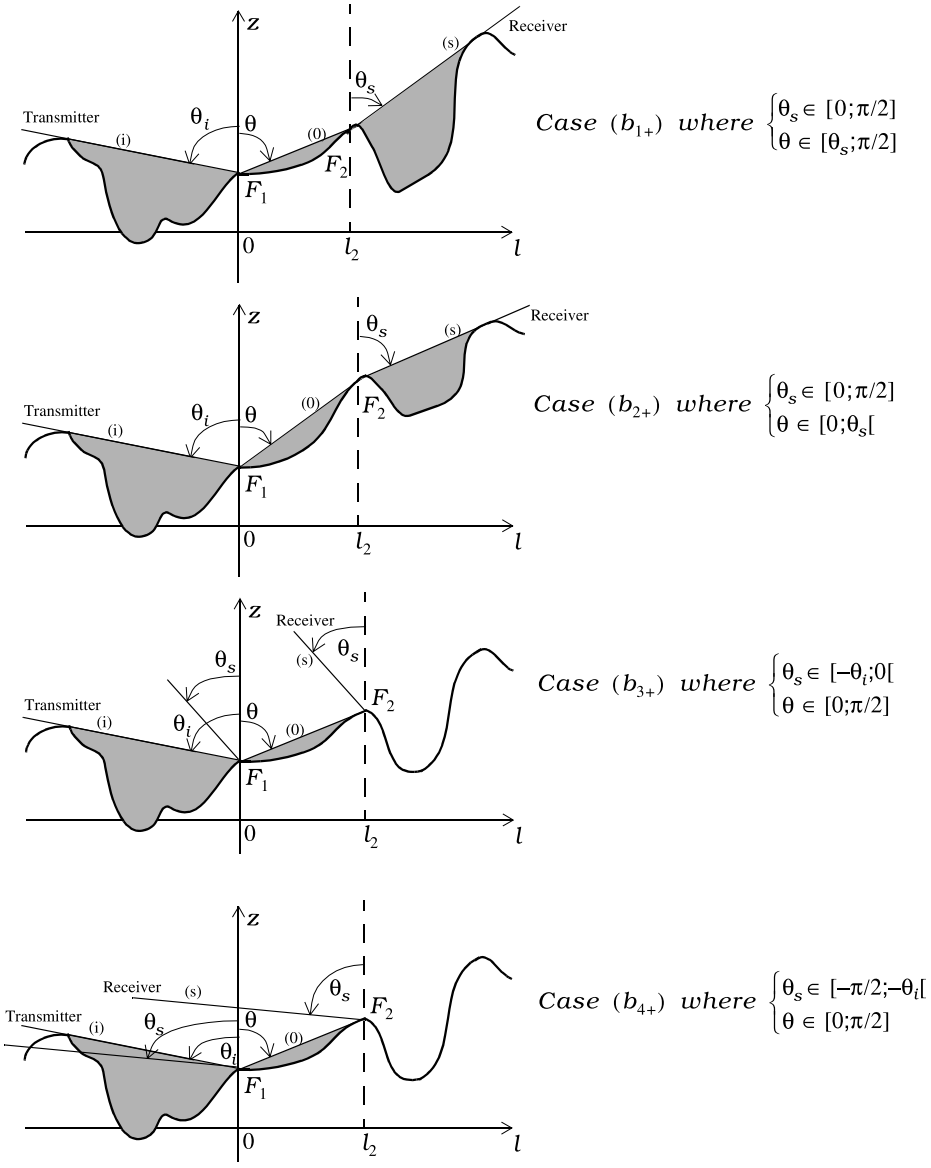


**Figure 7.** Bistatic statistical shadowing function with double reflection for $\theta_i \in [0; \pi/2], \theta \in [0; \pi/2]$ and $\theta_s \in [-\pi/2; \pi/2]$. The surface point $F_1(z_1, s_{1X})$ is characterized by the height $z_1$ and the slope $s_{1X}$, whereas the surface point $F_2(z_2, s_{2X})$ is described by $\{z_2, s_{2X}\}$. This figure depicts the case of the positive path.

where $F_i \equiv F_i(z_i, s_{iX})$. The cases $\{(b_{1+,2+,3+,4+})\}$ are defined with $\theta_i \in [0; \pi/2]$, and $\theta_s \in [-\pi/2; \pi/2]$ as (figure 7)

$$\begin{cases} \text{Case } (b_{1+}) & \text{where } \theta_s \in [0; \pi/2] & \text{and} & \theta \in [\theta_s; \pi/2] \\ \text{Case } (b_{2+}) & \text{where } \theta_s \in [0; \pi/2] & \text{and} & \theta \in [0; \theta_s[ \\ \text{Case } (b_{3+}) & \text{where } \theta_s \in [-\theta_i; 0[ & \text{and} & \theta \in [0; \pi/2] \\ \text{Case } (b_{4+}) & \text{where } \theta_s \in [-\pi/2; -\theta_i[ & \text{and} & \theta \in [0; \pi/2]. \end{cases} \tag{52a}$$

Since in (52), $\theta \in [0; \pi/2]$, the subscript + corresponds to the positive path. $S(\hat{\boldsymbol{K}}_i, \infty, F_1)$ represents the probability that the ray with incidence angle $\theta_i$ is not intercepted by the surface before it strikes the point $F_1(z_1, s_{1X})$. $\tilde{S}(\hat{\boldsymbol{K}}_+, l_2, F_1)$ denotes the probability that the ray (0) emanating from $F_1$ intercepts the surface at the point $F_2(z_2, s_{2X})$, where the symbol ˜ stands for the complementary probability ($\tilde{S} = 1 - S$). $S(\hat{\boldsymbol{K}}_s, \infty, F_2)$ is the probability that the ray ($s$) coming from $F_2$ is observed from the receiver. The contribution of the case ($b_{2+}$) is nil since the surface point $F_2$ cannot be viewed by the receiver. According to [12], we changed in (52) the probability $S(\hat{\boldsymbol{K}}_+, l_2, F_1)$ by $\tilde{S}(\hat{\boldsymbol{K}}_+, l_2, F_1)$.

$S(\hat{\boldsymbol{K}}, l_2, F_1)$ is the monostatic statistical shadowing function for a given observation length $l_2$. It is defined as

$$S(\hat{\boldsymbol{K}}, l_2, F_1) = S(\hat{\boldsymbol{K}}, F_1)[P_h(z_1 + \mu l_2) - P_h(-\infty)]^{-\Lambda(\hat{\boldsymbol{K}})} \quad \text{and} \quad S(\hat{\boldsymbol{K}}, \infty, F_1) = S(\hat{\boldsymbol{K}}, F_1), \tag{53}$$

where $S(\hat{\boldsymbol{K}}, F_1)$ and $\Lambda(\hat{\boldsymbol{K}})$ are given by (44$a$) and (44$b$).

For the coincidental waves, the incoherent scattering coefficient $\sigma_{2c}$ given by (41) requires the calculation of $\langle S_c(\hat{\boldsymbol{K}}_i, \hat{\boldsymbol{K}}_m, \hat{\boldsymbol{K}}_s | \boldsymbol{s}_1^{0c}, \boldsymbol{s}_2^{0c}, z_{21}) \exp[\pm \mathrm{j}(q - q')z_{21}] \rangle$. Using the same approach as mentioned previously, the knowledge of the surface slopes at the point (1) $\boldsymbol{s}_1^{0c}$ and (2) $\boldsymbol{s}_2^{0c}$ defined as (C5) implies that the angles $\{\theta_1, \theta_2\} \in \{]-\pi/2; \pi/2[\}$. Therefore, there is no restriction over the surface slopes and the monostatic statistical shadowing function $S(\hat{\boldsymbol{K}}, l_2, z_1, s_{1X})$ becomes $S(\hat{\boldsymbol{K}}, l_2, z_1)$, which is independent of the slopes $s_{1X}$. The average shadowing function is then expressed as

$$S_c(\hat{\boldsymbol{K}}_i, \hat{\boldsymbol{K}}_m, \hat{\boldsymbol{K}}_s | \boldsymbol{s}_1^{0c}, \boldsymbol{s}_2^{0c}) = \int_{-\infty}^{\infty} \mathrm{d}z_1 \int_{z_{2l}}^{z_{2u}} S_{2m}(\hat{\boldsymbol{K}}_i, \hat{\boldsymbol{K}}_m, \hat{\boldsymbol{K}}_s, z_1, z_2) p_h(z_1, z_2) \, \mathrm{d}z_2, \tag{54}$$

where $p_h(z_1, z_2)$ denotes the height joint probability separating two points on the surface of horizontal distance $l_2$. For the positive path, $\{z_{2l} = z_1, z_{2u} = \infty\}$, whereas for the negative path, $\{z_{2l} = -\infty, z_{2u} = z_1\}$. From figures 5 and 6, $l_2$ is equal to either $x_{12} \cos\varphi + y_{12} \sin\varphi$ or $x_{34} \cos\varphi + y_{34} \sin\varphi$. Since $\{x_{12}, x_{34}\}$ and $\{y_{12}, y_{34}\}$ are assumed to be greater than the surface correlation lengths $L_{cx}$ and $L_{cy}$, we get $p_h(z_1, z_2) \approx p_h(z_1) p_h(z_2)$. Hence, substituting (52) and (53) and into (54), we show from [12] that

$$\text{for } \varphi_s = \varphi_i, \qquad S_{2+}(\hat{\boldsymbol{K}}_i, \hat{\boldsymbol{K}}_+, \hat{\boldsymbol{K}}_s | \boldsymbol{s}_1^{0c}, \boldsymbol{s}_2^{0c}) \tag{55}$$

$$= \Lambda[(1 + \Lambda_i)(1 + \Lambda + \Lambda_i)(2 + \Lambda_i + \Lambda_s)]^{-1} \qquad \text{where } \theta_s \in [0; \pi/2], \tag{55$a$}$$

$$\Lambda[(1 + \Lambda_i)(1 + \Lambda + \Lambda_i)(2 + \Lambda_i)]^{-1} \qquad \text{where } \theta_s \in [-\theta_i; 0[, \tag{55$b$}$$

$$\Lambda[(1 + \Lambda_s)(1 + \Lambda + \Lambda_s)(2 + \Lambda_s)]^{-1} \qquad \text{where } \theta_s \in [-\pi/2; -\theta_i[. \tag{55$c$}$$

with

$$\Lambda_{i,s} = \Lambda(\hat{\boldsymbol{K}}_{i,s}), \Lambda = \Lambda(\hat{\boldsymbol{K}}_+). \tag{55$d$}$$

Since the surface is assumed to be even (the probability that the height $z \geqslant 0$ occurs is equal to the one obtained for $z \leqslant 0$), we show for the negative path that

$$S_{2-}(\hat{\boldsymbol{K}}_i, \hat{\boldsymbol{K}}_-, \hat{\boldsymbol{K}}_s | \boldsymbol{s}_1^{0c}, \boldsymbol{s}_2^{0c}) = S_{2+}(\hat{\boldsymbol{K}}_s, \hat{\boldsymbol{K}}_+, \hat{\boldsymbol{K}}_i | \boldsymbol{s}_1^{0c}, \boldsymbol{s}_2^{0c}). \tag{56}$$

This is similar to permute the transmitter with the receiver. For the case where $\varphi_s = \varphi_i + \pi_i$, the second-order illumination function is given by (55) and (56), where the ranges over $\theta_s$ are given by (49).

If the emitter and the receiver are in different planes $\{\varphi_s \neq \varphi_i, \varphi_s \neq \varphi_i + \pi\}$, then for any $\theta_s$ we have

$$S_{2+}\big(\hat{\boldsymbol{K}}_i, \hat{\boldsymbol{K}}_+, \hat{\boldsymbol{K}}_s \big| \boldsymbol{s}_1^{0c}, \boldsymbol{s}_2^{0c}\big) = \Lambda[(1+\Lambda_i)(1+\Lambda+\Lambda_i)(2+\Lambda_i+\Lambda_s)]^{-1} \quad \text{and equation (56).} \tag{57}$$

In fact, the ensemble average $S_c\big(\hat{\boldsymbol{K}}_i, \hat{\boldsymbol{K}}_m, \hat{\boldsymbol{K}}_s \big| \boldsymbol{s}_1^{0c}, \boldsymbol{s}_2^{0c}, z_{21}\big) \exp[\pm \mathrm{j}(q-q')z_{21}]$ is given rigorously by

$$\int_{-\infty}^{\infty} \mathrm{d}z_1 \int_{z_{2l}}^{z_{2u}} S_{2m}(\hat{\boldsymbol{K}}_i, \hat{\boldsymbol{K}}_m, \hat{\boldsymbol{K}}_s, z_1, z_2) \exp[\pm \mathrm{j}(q-q')z_{21}] p_h(z_1) p_h(z_2)\, \mathrm{d}z_2. \tag{58}$$

To compute this double integral analytically, the following assumption can be used:

$$\begin{aligned}\langle S_c \exp[\pm \mathrm{j}(q-q')z_{21}]\rangle &\approx \langle S_c\rangle_{z_2 \in [z_{2l}; z_{2u}]} \langle \exp[\pm \mathrm{j}(q-q')z_{21}]\rangle \\ &= S_{2m}(\hat{\boldsymbol{K}}_i, \hat{\boldsymbol{K}}_m, \hat{\boldsymbol{K}}_s) \langle \exp[\pm \mathrm{j}(q-q')z_{21}]\rangle. \end{aligned} \tag{59}$$

For a Gaussian process, $\langle \exp[\pm \mathrm{j}(q-q')z_{21}]\rangle = \exp\big[-(q-q')^2\sigma_h^2\big]$. Using the above equation leads to an overestimation of the modulus of the ensemble average (see appendix B of the companion paper).

The contribution of the anticoincidental waves $\sigma_{2a}$ given by (43) requires the derivation of $\big\langle S_a\big(\hat{\boldsymbol{K}}_i, \hat{\boldsymbol{K}}'_-, \hat{\boldsymbol{K}}_s \big| \boldsymbol{s}_1^{0a}, \boldsymbol{s}_2^{0a}, z_{21}\big) \exp[\,\mathrm{j}(q-q'-q_i-q_s)z_2]\big\rangle$. Using the same approach as mentioned previously, we have

$$\begin{aligned}\langle S_a \exp[\,\mathrm{j}(q-q'-q_i-q_s)z_{21}]\rangle &\approx \langle S_a\rangle \langle \exp[\,\mathrm{j}(q-q'-q_iq_s)z_{21}]\rangle \\ &= S_{2-}\big(\hat{\boldsymbol{K}}_i, \hat{\boldsymbol{K}}'_-\hat{\boldsymbol{K}}_s \big| \boldsymbol{s}_1^{0a}, \boldsymbol{s}_2^{0a}\big) \langle \exp[\,\mathrm{j}(q-q'-q_i-q_s)z_{21}]\rangle \\ &= S_{2-}\big(\hat{\boldsymbol{K}}_i, \hat{\boldsymbol{K}}'_-\hat{\boldsymbol{K}}_s \big| \boldsymbol{s}_1^{0c}, \boldsymbol{s}_2^{0c}\big) \langle \exp[\,\mathrm{j}(q-q'-q_i-q_s)z_{21}]\rangle. \end{aligned} \tag{60}$$

We can note that $S_{2-}\big(\hat{\boldsymbol{K}}_i, \hat{\boldsymbol{K}}'_-, \hat{\boldsymbol{K}}_s \big| \boldsymbol{s}_1^{0a}, \boldsymbol{s}_2^{0a}\big) = S_{2-}\big(\hat{\boldsymbol{K}}_i, \hat{\boldsymbol{K}}'_-, \hat{\boldsymbol{K}}_s \big| \boldsymbol{s}_1^{0c}, \boldsymbol{s}_2^{0c}\big)$ because there is no restriction over the surface slopes.

*4.2.3. Comparison with the formulations used by Ishimaru and Bahar.* Ishimaru and Bahar implicitly assumed that the shadowing effect is statistically independent of the surface elevations $\{\langle z_i\}$. The ensemble average $\langle\cdots\rangle$ over the surface elevations can be then written as $\langle\cdots\rangle = \langle\cdots\rangle_{\{z_i\}} \times \langle\cdots\rangle_{\{\Xi_1, \Xi_{2m}\}}$, where $\langle\cdots\rangle_{\{z_i\}}$ is the expected value by neglecting the shadowing effect and $\langle\cdots\rangle_{\{\Xi_1, \Xi_{2m}\}}$ denotes the second-order average shadowing function over the heights. In addition, $\langle\cdots\rangle_{\{\Xi_1, \Xi_{2m}\}}$ is calculated by a geometrical way by setting that

$$\langle\cdots\rangle_{\{\Xi_1, \Xi_{2m}\}} = S_1(\hat{\boldsymbol{K}}_i) \times [1 - S_1(\hat{\boldsymbol{K}})][1 - S_1(\hat{\boldsymbol{K}}')] \times S_1(\hat{\boldsymbol{K}}_s), \tag{61}$$

where $S_1$ is the monostatic average shadowing function with single reflection. Ishimaru used the Wagner formulation leading to $S_1(\hat{\boldsymbol{K}}) = [1 - \mathrm{erfc}(v)/2][1 - \mathrm{e}^{-\Lambda}/\Lambda]$ for a Gaussian process, where $\Lambda$ is calculated from (44*b*) and and $v = \cot\theta \big/ \big(2\langle s_{0X}^2\rangle\big)^{1/2}$. $(1 - \mathrm{e}^{-\Lambda})/\Lambda$ and $[1 - \mathrm{erfc}(v)/2]$ correspond to the average over the surface heights and slopes, respectively. Bahar used the Smith formulation by omitting the restriction over the surface slopes, which means that $S_1(\hat{\boldsymbol{K}}) = [1 + \Lambda]^{-1}$. Thus, comparing (61) with (55), there is no relation between these two approaches. Nevertheless, taking $\theta = \theta' = 90°$, we get $v = v' = 0$, $\Lambda(\hat{\boldsymbol{K}}) = \Lambda(\hat{\boldsymbol{K}}') \to \infty$, $S_1(\hat{\boldsymbol{K}}) = S_1(\hat{\boldsymbol{K}}') = 0$, $\langle\cdots\rangle_{\{\Xi_1, \Xi_{2m}\}} = [1 + \Lambda(\hat{\boldsymbol{K}}_i)]^{-1}[1 + \Lambda(\hat{\boldsymbol{K}}_s)]^{-1}$ with the Smith approach and $S_{2+}$ takes the form $[1 + \Lambda(\hat{\boldsymbol{K}}_i)]^{-1}[2 + \Lambda(\hat{\boldsymbol{K}}_s) + \Lambda(\hat{\boldsymbol{K}}_i)]^{-1}$ for $\theta_s \in [0; \pi/2]$, $[1 + \Lambda(\hat{\boldsymbol{K}}_{i,s})]^{-1}[2 + \Lambda(\hat{\boldsymbol{K}}_{i,s})]^{-1}$ else. If now $\theta_i = \theta_s = 0$ (there is no shadow for the transmitter and the receiver), then $\langle\cdots\rangle_{\{\Xi_1, \Xi_{2m}\}} = 1$ whereas $S_{2+} = 1/2$. Since for the positive path $z_{21} \geqslant 0$ and the surface is even (the probability that the height $z \geqslant 0$ occurs is equal to the one obtained for $z \leqslant 0$), the average over $z_{21}$ leads to the factor $1/2$

by neglecting the shadow. In conclusion, the ratio $S_{2+}/\langle\cdots\rangle_{\{\Xi_1,\Xi_{2m}\}}$ is of the order of $1/2$, which involves that the incoherent scattering coefficient follows approximately the same ratio. In fact, since Ishimaru *et al* expanded the Green function over $|x_2 - x_1|$, the factor $1/2$ is introduced within the integration over $x_{21} = x_2 - x_1$.

## 5. Conclusion

In this paper, for an anisotropic two-dimensional stationary rough surface assumed to be statistically even, the incoherent scattering coefficient with single and double reflections is calculated by taking into account the shadowing phenomenon. The model is obtained from the first- and second-order Kirchhoff approximation reduced to the geometric optics approximation, which assumes that the correlation between two adjacent points is very strong.

We show that the cross incoherent scattering coefficient is nil due to the shadow. The second-order scattered field is divided into two components related to the wave positive and negative paths, giving the contributions of the coincidental and anticoincidental waves of the incoherent scattering coefficient. This method then explains the origin of the backscattering enhancement. The second-order incoherent scattering coefficient is then proportional to the product of two surface slope probabilities for which the slopes would specularly reflect the rays in the double scattering process. In addition, the slope distributions are related to each other by a propagating term, equal to the modified characteristic function derived over the elevation difference where both reflections occur. This result generalizes the one obtained by Sancer [16] for any process in the case of single scattering. The propagating term also takes into account the shadowing effect in the double-scattering phenomenon and includes the probability that a ray emanating from the first reflection intercepts the surface in order to give the second reflection. This probability is obtained from the shadowing function with double reflection calculated for any even process.

In the companion paper, the present model will be simulated and compared with numerical results.

### Acknowledgments

The authors thank the referees for their relevant comments.

## Appendix A. Polarization terms for the first-order Kirchhoff approximation

According to the polarization states of the incident $i = \{v_i, h_i\}$ and scattered $s = \{v_s, h_s\}$ fields, the elements of the matrix $\bar{F}_1(\hat{\boldsymbol{K}}_i, \hat{\boldsymbol{K}}_s)$ are expressed from [15] as

$$\bar{F}_1 = \begin{bmatrix} F_1^{v_i v_s} & F_1^{v_i h_s} \\ F_1^{h_i v_s} & F_1^{h_i h_s} \end{bmatrix}, \tag{A1}$$

where

$$\begin{cases} F_1^{v_i v_s}(\hat{\boldsymbol{K}}_i, \hat{\boldsymbol{K}}_s) = D(f_2 F_V + f_1 F_H) \\ F_1^{v_i h_s}(\hat{\boldsymbol{K}}_i, \hat{\boldsymbol{K}}_s) = D(f_3 F_V - f_4 F_H) \\ F_1^{h_i v_s}(\hat{\boldsymbol{K}}_i, \hat{\boldsymbol{K}}_s) = D(f_4 F_V - f_3 F_H) \\ F_1^{h_i h_s}(\hat{\boldsymbol{K}}_i, \hat{\boldsymbol{K}}_s) = D(f_1 F_V + f_2 F_H) \end{cases} \qquad \begin{cases} f_1 = (\hat{\boldsymbol{h}}_s \cdot \hat{\boldsymbol{K}}_i)(\hat{\boldsymbol{h}}_i \cdot \hat{\boldsymbol{K}}_s) \\ f_2 = (\hat{\boldsymbol{v}}_s \cdot \hat{\boldsymbol{K}}_i)(\hat{\boldsymbol{v}}_i \cdot \hat{\boldsymbol{K}}_s) \\ f_3 = (\hat{\boldsymbol{v}}_s \cdot \hat{\boldsymbol{K}}_i)(\hat{\boldsymbol{h}}_i \cdot \hat{\boldsymbol{K}}_s) \\ f_4 = (\hat{\boldsymbol{h}}_s \cdot \hat{\boldsymbol{K}}_i)(\hat{\boldsymbol{v}}_i \cdot \hat{\boldsymbol{K}}_s) \\ D = q_1^2 \big/ \{q_{1z}[(\hat{\boldsymbol{h}}_s \cdot \hat{\boldsymbol{K}}_i)^2 + (\hat{\boldsymbol{v}}_s \cdot \hat{\boldsymbol{K}}_i)^2]\}, \end{cases} \tag{A2}$$

where the scalar products are calculated from (4) and (5)

$$\begin{cases} \hat{\boldsymbol{h}}_s \cdot \hat{\boldsymbol{K}}_i = -\sin\theta_i \sin(\varphi_s - \varphi_i) \\ \hat{\boldsymbol{h}}_i \cdot \hat{\boldsymbol{K}}_s = \sin\theta_s \sin(\varphi_s - \varphi_i), \end{cases} \tag{A3}$$

$$\begin{cases} \hat{\boldsymbol{v}}_s \cdot \hat{\boldsymbol{K}}_i = \sin\theta_i \cos\theta_s \cos(\varphi_s - \varphi_i) + \cos\theta_i \sin\theta_s \\ \hat{\boldsymbol{v}}_i \cdot \hat{\boldsymbol{K}}_s = -[\sin\theta_s \cos\theta_i \cos(\varphi_s - \varphi_i) + \cos\theta_s \sin\theta_i], \end{cases} \tag{A4}$$

and

$$q_{1z} = \cos\theta_i + \cos\theta_s, \tag{A5}$$

$$q_1 = \{2[1 + \cos\theta_i \cos\theta_s - \sin\theta_i \sin\theta_s \cos(\varphi_s - \varphi_i)]\}^{1/2}. \tag{A6}$$

The Fresnel coefficients $\{F_{V,H}\}$ are performed with an incidence angle $\theta_{10} = -\arccos(\hat{\boldsymbol{N}}_{10} \cdot \hat{\boldsymbol{K}}_i)$, where

$$\hat{\boldsymbol{N}}_{10} \cdot \hat{\boldsymbol{K}}_i = [(\hat{\boldsymbol{K}}_s - \hat{\boldsymbol{K}}_i) \cdot \hat{\boldsymbol{K}}_i]/\|\hat{\boldsymbol{K}}_s - \hat{\boldsymbol{K}}_i\| = -q_1/2. \tag{A7}$$

## Appendix B. Derivation of the cross incoherent scattering coefficient

This appendix is devoted to the derivation of the cross incoherent scattering coefficient expressed from (30).

In (30*a*), the random variables are $\{\Xi_{2m}, \Xi_1, \boldsymbol{s}_2, z_{21} = z_2 - z_1\}$. We can show that the covariance matrix of samples $\{\boldsymbol{s}_2, z_{21}\} = \{s_{2x}, s_{2y}, z_{21}\}$ is

$$[C_{12}] = \begin{bmatrix} \sigma_{sx}^2 & 0 & -\rho_{1x} \\ 0 & \sigma_{sy}^2 & -\rho_{1y} \\ -\rho_{1x} & -\rho_{1y} & 2\left(\sigma_h^2 - \rho_0\right) \end{bmatrix}, \tag{B1}$$

where

$$\rho_{1x} = \frac{\partial \rho_0}{\partial x_{21}} \qquad \rho_{1y} = \frac{\partial \rho_0}{\partial y_{21}} \qquad \rho_{2xy} = \frac{\partial^2 \rho_0}{\partial x_{21} \partial y_{21}}. \tag{B2}$$

In the above equations $\left\{\sigma_{sx}^2, \sigma_{sy}^2\right\} = \{-\rho_{2x}(\mathbf{O}), -\rho_{2y}(\mathbf{O})\}$ are the surface slope variances along the directions $\{\hat{\boldsymbol{x}}, \hat{\boldsymbol{y}}\}$ and $\sigma_h^2 = \rho_0(\mathbf{O})$ is the height variance. $\rho_0(\mathbf{r}_{21})$ stands for the height correlation function, assumed to be even ($\rho_0(\pm\mathbf{r}_{21}) = \rho_0(\mathbf{r}_{21})$). It should be noted that $\langle s_{2x} z_2 \rangle = \rho_{1x}(\mathbf{O}) = 0$, $\langle s_{2y} z_2 \rangle = \rho_{1y}(\mathbf{O}) = 0$ and $\langle s_{2x} s_{2y} \rangle = -\rho_{2xy}(\mathbf{O}) = 0$ since $\{\rho_{1x}, \rho_{1y}, \rho_{2xy}\}$ are odd.

Since $[C_{12}]$ is independent of $\mathbf{r}_{32}$ and the integration limit over $\mathbf{r}_{32}$ can be extended to $\pm\infty$, the integration over $\mathbf{r}_{32}$ of (30*a*) leads to

$$A_{12} = (2\pi)^2 \int_{S_0} \mathrm{d}\mathbf{r}_{21} \langle \Xi_{2m}(\mathbf{r}_1, \mathbf{r}_2) \Xi_1(\mathbf{r}_3) \delta(\boldsymbol{k}_s - \boldsymbol{k}_i + \boldsymbol{s}_2[q_s - q_i]) \times \exp\{\mathrm{j}(\boldsymbol{k} - \boldsymbol{k}_i) \cdot \mathbf{r}_{21} + z_{21}(mq - q_i)\}\rangle. \tag{B3}$$

As previously mentioned, it is convenient to represent the density function $p(\boldsymbol{s}_2, z_{21}, \Xi_1, \Xi_{2m})$ in terms of the conditional probability as

$$p(\boldsymbol{s}_2, z_{21}, \Xi_1, \Xi_{2m}) = p(\boldsymbol{s}_2, z_{21}) \times p(\Xi_1, \Xi_{2m} | \boldsymbol{s}_2, z_{21}), \tag{B4}$$

where

$$p(\boldsymbol{s}_2, z_{21}, \Xi_1, \Xi_{2m}) = S_{12}(\hat{\boldsymbol{K}}_i, \hat{\boldsymbol{K}}_s, \hat{\boldsymbol{K}}_m | \boldsymbol{s}_2, z_{21}) \delta(\Xi_{12m} - 1) + [1 - S_{12}(\hat{\boldsymbol{K}}_i, \hat{\boldsymbol{K}}_s, \hat{\boldsymbol{K}}_m | \boldsymbol{s}_2, z_{21})] \delta_2(\Xi_{12m}), \tag{B5}$$

and $\Xi_{12m} = [\Xi_1 \Xi_{2m}]$ is a vector of length 2. Substituting (B5) and (B4) into (B3), and calculating the ensemble average over the slope $\boldsymbol{s}_2$, we obtain

$$A_{12} = \left(\frac{2\pi}{q_s - q_i}\right)^2 \int_{S_0} \mathrm{d}\mathbf{r}_{21} \exp[\,\mathrm{j}(\boldsymbol{k} - \boldsymbol{k}_i)\cdot\mathbf{r}_{21}]\left\langle S_{12}(\hat{\boldsymbol{K}}_i, \hat{\boldsymbol{K}}_s, \hat{\boldsymbol{K}}_m \big| \boldsymbol{s}_2^0, z_{21}\right) \times \exp[\,\mathrm{j}z_{21}(mq - q_i)]\Big\rangle, \tag{B6}$$

where

$$\boldsymbol{s}_2^0 = -(\boldsymbol{k}_s - \boldsymbol{k}_i)/(q_s - q_i). \tag{B7}$$

Thus, the only random variable is $z_{21}$. To simplify $\sigma_{12}$, the correlation between the points (1) and (2) is omitted, which means $\rho_0 \approx 0$. The double scattering process consists of a pair of slopes defined at the points (1) and (2), whose values are appreciably different. But the slopes along the $\{\hat{\boldsymbol{x}}, \boldsymbol{y}\}$ directions of a random surface change significantly in the correlation distances $\{L_{cx}, L_{cy}\}$. Thus, we expect $\{|x_{21}| > L_{cx}, |y_{21}| > L_{cy}\}$ for a typical case, therefore the correlation between $z_2$ and $z_1$ can be omitted. This implies that the covariance matrix given by (B1) becomes diagonal. The substitution of (B6) into (30) then yields

$$\sigma_{12} = \frac{\pi k_0^2 p_s(\boldsymbol{s}_2^0)}{4(q_s - q_i)^2} \Re\left\{ \bar{F}_1{}^*(\hat{\boldsymbol{K}}_i, \hat{\boldsymbol{K}}_s) \int \frac{\bar{F}_{1m}(\hat{\boldsymbol{K}}_i, \hat{\boldsymbol{K}}_m, \hat{\boldsymbol{K}}_s)\chi_t(\boldsymbol{k} - \boldsymbol{k}_i)}{q} \times \left\langle S_{12}\left(\hat{\boldsymbol{K}}_i, \hat{\boldsymbol{K}}_s, \hat{\boldsymbol{K}}_m \big| \boldsymbol{s}_2^0, z_{21}\right) \exp[\,\mathrm{j}z_{21}(mq - q_i)]\right\rangle \mathrm{d}\boldsymbol{k} \right\}, \tag{B8}$$

where

$$\chi_t(\boldsymbol{u}) = \left(\frac{k_0}{\pi}\right)^2 \int S_t(\boldsymbol{u}) \exp(\,\mathrm{j}\boldsymbol{u}\cdot\mathbf{r}_{21})\,\mathrm{d}\mathbf{r}_{21} \quad \text{and} \quad \left\langle z_{21}^2 \right\rangle = 2\sigma_h^2. \tag{B9}$$

$S_t(\boldsymbol{u})$ is a tapering function which quantifies the fact that the scattered waves at the point (1) propagate only in a certain distance before being intercepted at the point (2) by the surface. It will be expressed in the companion paper. In (B8), the integration range of $\boldsymbol{k}$ is $\{]-\infty; \infty[\}$. To be consistent with the geometric optics approximation, the evanescent waves are omitted, which involves from appendix D that $\|\boldsymbol{k}\| \in [-k_0; k_0]$. In the spherical coordinates, where the components of $\{\hat{\boldsymbol{K}}_i, \hat{\boldsymbol{K}}_m, \hat{\boldsymbol{K}}_s\}$ are given by (4), (5) and (7*a*), we then obtain

$$\sigma_{12} = \frac{\pi k_0^2 p_s(\boldsymbol{s}_2^0)}{4(q_s - q_i)^2} \Re\left\{ \bar{F}_1{}^*(\hat{\boldsymbol{K}}_i, \hat{\boldsymbol{K}}_s) \int_0^{\pi/2} \sin\theta\,\mathrm{d}\theta \int_0^{2\pi} \bar{F}_{1m}(\hat{\boldsymbol{K}}_i, \hat{\boldsymbol{K}}_m, \hat{\boldsymbol{K}}_s)\chi_t(\boldsymbol{k} - \boldsymbol{k}_i) \times \left\langle S_{12}\left(\hat{\boldsymbol{K}}_i, \hat{\boldsymbol{K}}_s, \hat{\boldsymbol{K}}_m \big| \boldsymbol{s}_2^0, z_{21}\right) \exp[\,\mathrm{j}z_{21}(mq - q_i)]\right\rangle \mathrm{d}\varphi \right\}. \tag{B10}$$

## Appendix C. Derivation of the second-order incoherent scattering coefficient

This appendix is devoted to the derivation of the second-order incoherent scattering coefficient expressed from (40) giving the contribution of the coincidental waves.

The random variables in (39) are $\{\Xi_{2\pm}, \Xi'_{2\pm}, \boldsymbol{s}_1, \boldsymbol{s}_2, z_{21}\}$. The covariance matrix of samples $\{s_{1x}, s_{2x}, s_{1y}, s_{2y}, z_{21}\}$ is

$$[C_c] = \begin{bmatrix} \sigma_{sx}^2 & -\rho_{2x} & 0 & -\rho_{2xy} & -\rho_{1x} \\ -\rho_{2x} & \sigma_{sx}^2 & -\rho_{2xy} & 0 & -\rho_{1x} \\ 0 & -\rho_{2xy} & \sigma_{sy}^2 & -\rho_{2y} & -\rho_{1y} \\ -\rho_{2xy} & 0 & -\rho_{2y} & \sigma_{sy}^2 & -\rho_{1y} \\ -\rho_{1x} & -\rho_{1x} & -\rho_{1y} & -\rho_{1y} & 2(\sigma_h^2 - \rho_0) \end{bmatrix}. \tag{C1}$$

where $\{\rho_{1x}, \rho_{1y}, \rho_{2xy}\}$ are defined as (B2) and

$$\rho_{2x} = \frac{\partial^2 \rho_0}{\partial x_{21}^2} \qquad \rho_{2y} = \frac{\partial^2 \rho_0}{\partial y_{21}^2}. \tag{C2}$$

Since the height correlation $\rho_0(\mathbf{r}_{21})$ is even ($\rho_0(\pm\mathbf{r}_{21}) = \rho_0(\mathbf{r}_{21})$), $\{\rho_{1x}, \rho_{1y}, \rho_{2xy}\}$ are odd, which implies that $\rho_{1x,1y,2xy}(\mathbf{O}) = 0$. For instance, this explains that $\langle s_{1x,1y} z_{21}\rangle = \langle s_{1x,1y} z_2\rangle - \langle s_{1x,1y} z_1\rangle = -\rho_{1x,1y} + \rho_{1x,1y}(\mathbf{O}) = -\rho_{1x,1y}$. In addition, $\{-\rho_{2x}(\mathbf{O}), -\rho_{2y}(\mathbf{O})\} = \left\{\sigma_{sx}^2, \sigma_{sy}^2\right\}$ are the surface slope variances along the directions $\{\hat{\boldsymbol{x}}, \hat{\boldsymbol{y}}\}$ and $\sigma_h^2 = \rho_0(\mathbf{O})$ is the height variance.

In view of (38) and (39), since the covariance matrix is independent of $\{\mathbf{r}_{31}, \mathbf{r}_{24}\}$, the integrations over $\{\mathbf{r}_{31}, \mathbf{r}_{24}\}$ of (40*a*), where the integrations limit can be extended to $\mp\infty$, lead to

$$A_2 = (2\pi)^4 \int_{S_0} \exp[\,\mathrm{j}(\boldsymbol{k} - \boldsymbol{k}') \cdot \mathbf{r}_{21}] \langle \Xi_{2\pm} \Xi'_{2\pm} \exp[\pm \mathrm{j}(q - q') z_{21}] \\ \times \delta([\pm q' - q_i]\boldsymbol{s}_1 + \boldsymbol{k}' - \boldsymbol{k}_i) \delta([\pm q' - q_s]\boldsymbol{s}_2 + \boldsymbol{k}' - \boldsymbol{k}_s) \rangle \mathrm{d}\mathbf{r}_{21}. \tag{C3}$$

Using the same form as (B4) and (B5), the calculation of the expected value over $\{\boldsymbol{s}_1, \boldsymbol{s}_2\}$ yields

$$A_2 = \frac{(2\pi)^4}{(\pm q' - q_i)^2 (\pm q' - q_s)^2} \int_{S_0} \exp[\,\mathrm{j}(\boldsymbol{k} - \boldsymbol{k}') \cdot \mathbf{r}_{21}] \left\langle S_c\left(\hat{\boldsymbol{K}}_i, \hat{\boldsymbol{K}}_m, \hat{\boldsymbol{K}}_s \middle| \boldsymbol{s}_1^{0c}, \boldsymbol{s}_2^{0c}, z_{21}\right) \right. \\ \left. \times \exp[\pm \mathrm{j}(q - q') z_{21}] \right\rangle \mathrm{d}\mathbf{r}_{21}, \tag{C4}$$

where

$$\boldsymbol{s}_1^{0c} = -(\boldsymbol{k}' - \boldsymbol{k}_i)/(\pm q' - q_i), \qquad \boldsymbol{s}_2^{0c} = -(\boldsymbol{k}' - \boldsymbol{k}_s)/(\pm q' - q_s). \tag{C5}$$

$S_c$ is the second-order illumination function with the knowledge of $\left\{\boldsymbol{s}_1^{0c}, \boldsymbol{s}_2^{0c}\right\}$. This function is presented in subsection 4.2.2. As previously mentioned, it is reasonable to neglect the correlation between the points (1) and (2). The covariance matrix given by (C1) then becomes diagonal, and we have for any random process

$$p(\boldsymbol{s}_1, \boldsymbol{s}_2, z_{21}) = p_s(\boldsymbol{s}_1) p_s(\boldsymbol{s}_2) p_h(z_{21}). \tag{C6}$$

Therefore, substituting (C6) into (C4) and into (40), omitting the evanescent waves (see appendix D), the incoherent scattering coefficient takes the form

$$\sigma_{2c} = \frac{\pi k_0^4}{16} \int_0^{\pi/2} \mathrm{d}\theta \int_0^{\pi/2} \mathrm{d}\theta' \int_0^{2\pi} \mathrm{d}\varphi \int_0^{2\pi} \mathrm{d}\varphi' \frac{|\bar{F}_{1m}(\hat{\boldsymbol{K}}_i, \hat{\boldsymbol{K}}'_m, \hat{\boldsymbol{K}}_s)|^2 \chi_t(\boldsymbol{k} - \boldsymbol{k}') \sin\theta \sin\theta'}{(\pm q' - q_i)^2 (\pm q' - q_s)^2} \\ \times p_s\left(\boldsymbol{s}_1^{0c}\right) p_s\left(\boldsymbol{s}_2^{0c}\right) \left\langle S_c\left(\hat{\boldsymbol{K}}_i, \hat{\boldsymbol{K}}_m, \hat{\boldsymbol{K}}_s \middle| \boldsymbol{s}_1^{0c}, \boldsymbol{s}_2^{0c}, z_{21}\right) \exp[\pm \mathrm{j}(q - q') z_{21}] \right\rangle. \tag{C7}$$

## Appendix D. Weyl's representation

This appendix discusses the origin of the evanescent waves from the Weyl representation of the scalar Green function.

Using the polar coordinates $\{k_x = \kappa \cos\varphi, k_y = \kappa \sin\varphi\}$, (10) can be expressed as

$$G(\boldsymbol{R}_1, \boldsymbol{R}_2) = \frac{\mathrm{j}}{8\pi^2} \int_0^{\infty} \frac{\exp(\,\mathrm{j}q|z_2 - z_1|)\,\mathrm{d}\kappa}{q} \left\{ \int_0^{2\pi} \exp[\,\mathrm{j}\kappa \|\mathbf{r}_{21}\| \cos(\varphi - \phi_\kappa)]\,\mathrm{d}\varphi \right\} \\ \text{with} \qquad q = \begin{cases} \left(k_0^2 - \kappa^2\right)^{1/2} & \text{if } k_0^2 \geqslant \kappa^2 \\ j\left(\kappa^2 - k_0^2\right)^{1/2} & \text{if } k_0^2 < \kappa^2, \end{cases} \tag{D1}$$

where

$$\phi_\kappa = \arctan[(y_2 - y_1)/(x_2 - x_1)]. \tag{D2}$$

The integration over $\varphi$ gives ($\|\mathbf{r}_{21}\| = r_{21}$)

$$G(\boldsymbol{R}_1, \boldsymbol{R}_2) = \frac{\mathrm{j}}{4\pi} \int_0^\infty \frac{\mathrm{d}\kappa}{q} J_0(\kappa r_{21}) \exp(\mathrm{j}q|z_2 - z_1|), \tag{D3}$$

where $J_0$ is the Bessel function of the first kind and zero order. According to the value of $\kappa$, we can expand the above equation as

$$\begin{aligned} G(\boldsymbol{R}_1, \boldsymbol{R}_2) = {} & \frac{\mathrm{j}}{4\pi} \int_0^{k_0} \mathrm{d}\kappa \frac{J_0(\kappa r_{21}) \exp\left[\mathrm{j}\left(k_0^2 - \kappa^2\right)^{1/2}|z_2 - z_1|\right]}{\left(k_0^2 - \kappa^2\right)^{1/2}} \\ & + \frac{1}{4\pi} \int_{k_0}^\infty \mathrm{d}\kappa \frac{J_0(\kappa r_{21}) \exp\left[-\left(\kappa^2 - k_0^2\right)^{1/2}|z_2 - z_1|\right]}{\left(\kappa^2 - k_0^2\right)^{1/2}}. \end{aligned} \tag{D4}$$

In the first and second terms of (D4) right-hand side, using the variable transformations $x = \left(1 - \kappa^2/k_0^2\right)^{1/2}$, $x = \left(\kappa^2/k_0^2 - 1\right)^{1/2}$ leads to

$$\begin{aligned} G(\boldsymbol{R}_1, \boldsymbol{R}_2) = {} & \frac{\mathrm{j}k_0}{4\pi} \int_0^1 J_0\left(\left[k_0^2(1 - x^2)\right]^{1/2} r_{21}\right) \exp(\mathrm{j}k_0 x|z_2 - z_1|)\,\mathrm{d}x \\ & + \frac{k_0}{4\pi} \int_0^\infty J_0\left(\left[k_0^2(1 + x^2)\right]^{1/2} r_{21}\right) \exp(-k_0 x|z_2 - z_1|)\,\mathrm{d}x. \end{aligned} \tag{D5}$$

Since $k_0$ is real for the air, the second term of (D5) right-hand side represents the evanescent waves. In this paper these modes are neglected. Therefore, in spherical coordinates, the scalar Green function given by (10) can be expressed as

$$\begin{aligned} G(\boldsymbol{R}_1, \boldsymbol{R}_2) = {} & \frac{\mathrm{j}k_0}{8\pi^2} \int_0^{\pi/2} \sin\theta\,\mathrm{d}\theta \int_0^{2\pi} \exp\{\mathrm{j}k_0[(x_2 - x_1)\sin\theta\cos\varphi \\ & + (y_2 - y_1)\sin\varphi\sin\varphi + \cos\theta|z_2 - z_1|]\}\,\mathrm{d}\varphi, \end{aligned} \tag{D6}$$

where the evanescent waves are omitted (case where $\boldsymbol{k}^2 > k_0^2$).

## References


[1] Ishimaru A 1991 Backscattering enhancement: from radar cross sections to electron and light localizations to roughsurface scattering *IEEE Antennas Propag. Mag.* **33** 7–11

[2] O'Donnell K A and Mendez E R 1987 Experimental study of scattering from characterized random surfaces *J. Opt. Soc. Am.* A **4** 1194–205

[3] Kim M J, Sant A J and Friberg J C 1990 Experimental study of enhanced backscattering from one- and two-dimensional surfaces *J. Opt. Soc. Am.* A **4** 569–77

[4] Dainty J C, Bruce N C and Sant A J 1991 Measurements of light scattering by a characterizing random rough surface *Waves Random Media* **3** S29–39

[5] Knotts M E and O'Donnell K A 1994 Measurements of light scattering by a series of conducting surfaces with one-dimensional roughness *J. Opt. Soc. Am.* A **11** 697–710

[6] Jonhson J T, Tsang L, Shin R T, Pak K, Chan C H, Ishimaru A and Kuga Y 1996 Backscattering enhancement of electromagnetics waves from two-dimensional perfectly conducting random rough surfaces: a comparison of Monte Carlo simulations with experimental data *IEEE Trans. Antennas Propag.* **11** 748–56

[7] Tsang L, Kong J A, Ding K-H and On Ao C 2001 *Scattering of Electromagnetic Waves. Numerical Solutions* (New York: Wiley)

[8] Torrungrueng D and Johnson J T 2001 Numerical studies of backscattering enhancement of electromagnetic waves from two-dimensional random rough surfaces with the forward-backward/novel spectral acceleration method *JOSA* A **18** 2518–26

[9] Ishimaru A, Le C, Kuga Y, Sengers L A and Chan T K 1996 Polarimetric scattering theory for high slope rough surfaces *Prog. Electromagn. Res.* **14** 1–36
[10] Hsieh C Y 2000 Prediction of IEM model for backscattering enhancement *Electromagnetics* **20** 205–31
[11] Bahar E and El-Shenawee M 2001 Double-scatter cross sections for two-dimensional random rough surfaces that exhibit backscatter enhancement *JOSA* A **18** 108–16
[12] Bourlier C, Berginc G and Saillard J 2002 Monostatic and bistatic statistical shadowing functions from a one-dimensional stationary randomly rough surface: II. Multiple scattering *Waves Random Media* **12** 175–200
[13] Alvarez-Pérez J L 2001 An extension of the IEM/IEMM surface scattering model *Waves Random Media* **11** 307–29
[14] Fung A K 1994 *Microwave Scattering and Emission Models and their Applications* (Boston MA: Artech House)
[15] Ulaby F T, Moore R K and Fung A K 1982 *Microwave Remote Sensing* vol II (Reading, MA: Addison-Wesley)
[16] Sancer M I 1969 Shadow-corrected electromagnetic scattering from a randomly rough surface *IEEE Trans. Antennas Propag.* **17** 577–85
[17] Bourlier C, Berginc G and Saillard J 2002 One- and two-dimensional shadowing functions for any height and slope stationary uncorrelated surface in the monostatic and bistatic configurations *IEEE Trans. Antennas Propag.* **50** 312–24
[18] Bourlier C and Berginc G 2003 Shadowing function with single reflection from anisotropic Gaussian rough surface. Application to Gaussian, Lorentzian and sea correlations *Waves Random Media* **13** 27–58